Check for updates

ARTICLE

Gut microbiota drives macrophage-dependent self-renewal of intestinal stem cells via niche enteric serotonergic neurons

Pingping Zhu [1,2,3,9 ✉], Tiankun Lu[1,4,9], Jiayi Wu[1,5,9], Dongdong Fan[6,9], Benyu Liu[1,7], Xiaoxiao Zhu[6], Hui Guo[1], Ying Du[1], Feng Liu [8], Yong Tian [4,6 ✉] and Zusen Fan [1,4 ✉]

Lgr5[+] intestinal stem cells (ISCs) reside within specialized niches at the crypt base and harbor self-renewal and differentiation capacities. ISCs in the crypt base are sustained by their surrounding niche for precise modulation of self-renewal and differentiation. However, how intestinal cells in the crypt niche and microbiota in enteric cavity coordinately regulate ISC stemness remains unclear. Here, we show that ISCs are regulated by microbiota and niche enteric serotonergic neurons. The gut microbiota metabolite valeric acid promotes *Tph2* expression in enteric serotonergic neurons via blocking the recruitment of the NuRD complex onto *Tph2* promoter. 5-hydroxytryptamine (5-HT) in turn activates PGE2 production in a PGE2^{+} macrophage subset through its receptors HTR2A/3 A; and PGE2 via binding its receptors EP1/EP4, promotes Wnt/β-catenin signaling in ISCs to promote their self-renewal. Our findings illustrate a complex crosstalk among microbiota, intestinal nerve cells, intestinal immune cells and ISCs, revealing a new layer of ISC regulation by niche cells and microbiota.

INTRODUCTION

The intestine is the largest digestive and absorptive organ, consisting of intestinal epithelium, lamina propria, muscle and so on. Intestine epithelium, the most frequently renewing organ in adult mammals, contains five kinds of mature cells, including enterocytes, goblet cells, enteroendocrine cells, Paneth cells and tuft cells.[1] All these mature cells are derived from Lgr5^{+} intestinal stem cells (ISCs), which reside at the crypt base and harbor self-renewal and differentiation capacities.[2] Many signaling pathways participate in the regulation of self-renewal and multipotency of Lgr5^{+} ISCs, including Wnt/β-catenin signaling, Notch signaling, BMP signaling, ErbB signaling and Hedgehog signaling.[3] The self-renewal of ISCs is under precise regulation by numerous intracellular and extracellular signals. Recently, we identified an ISC-intracellular long noncoding RNA lncGata6 required for ISC self-renewal.[4] The extracellular niche provides Wnt, Notch and epidermal growth factor (EGF) signals to support ISC self-renewal and normal epithelial maintenance.[5,6] Numerous kinds of cells have been identified as niche cells for ISCs. In the small intestine, ISCs are interspersed between Paneth cells, which secrete critical molecules such as Wnt3, EGF, Notch, lactate and cyclic ADP ribose to maintain the stemness of ISCs.[6–8] Stroma cells, FOXL1^{+} subepithelial telocytes and CD90^{+}CD81^{+}CD34^{+}CD138^{-} MAP3K2-regulated intestinal stromal cells (MRISCs) also provide Wnt and Rspo ligands as ISC niche cells.[9,10] However, it is still elusive to comprehensively define ISC niche cells and niche factors.

The ISC niche contains two major components: extracellular matrix (ECM) and cellular microenvironment. The cellular micro-environment comprises all the resident cells embedded within the ECM, including pericryptal myofibroblasts, fibroblasts, pericytes, endothelial cells, immune cells, neural cells, and smooth muscle cells. These cells secrete a wide range of matrix components and growth factors for the regulation of ISC self-renewal and differentiation.[11,12] Accumulating evidence demonstrates critical roles of immune cells in ISC self-renewal. For example, T cells from allogeneic transplantation mainly locate in ISC compartment and kill ISCs, which express MHC class I and II molecules.[13] IL-22 secreted by group 3 ILCs (ILC3s) can promote ISC-mediated epithelial regeneration after intestinal damage, and drive ISC self-renewal.[14] Recently, we revealed that ILC2 cells promote ISC self-renewal via IL-13 pathway.[15]

Besides immune cells, the intestinal tract contains an intrinsic nervous system that is termed as the enteric nervous system (ENS). The total number of enteric neurons is 400–600 million in human and almost equal to the number of neurons in spinal cord.[16] The ENS regulates the behavior of the gut and connects to the central nervous system (CNS).[17] However, it remains unclear whether nerve cells, the extremely enriched cells in intestines, can regulate ISC self-renewal. 5-hydroxytryptamine (5-HT), also known as serotonin, plays important roles in enteric neurotransmission, initiation and propagation of intrinsic enteric reflexes, gut-to-brain connections, as well as many other biological processes.[18] Within

[1]CAS Key Laboratory of Infection and Immunity, CAS Center for Excellence in Biomacromolecules, Institute of Biophysics, Chinese Academy of Sciences, Beijing, China. [2]School of Life Sciences, Zhengzhou University, Zhengzhou, Henan, China. [3]State Key Laboratory of Esophageal Cancer Prevention & Treatment, Zhengzhou University, Zhengzhou, Henan, China. [4]University of Chinese Academy of Sciences, Beijing, China. [5]School of Medicine, Nankai University, 94 Weijin Road, Tianjin, China. [6]CAS Key Laboratory of RNA Biology; Institute of Biophysics, Chinese Academy of Sciences, Beijing, China. [7]Research Center of Basic Medicine, Academy of Medical Sciences, Zhengzhou University, Zhengzhou, Henan, China. [8]State Key Laboratory of Membrane Biology, Institute of Zoology, Chinese Academy of Sciences, Beijing, China. [9]These authors contributed equally: Pingping Zhu, Tiankun Lu, Jiayi Wu, Dongdong Fan. ✉email: zhup@zzu.edu.cn; ytian@ibp.ac.cn; fanz@moon.ibp.ac.cn

556

the gut, 5-HT is synthesized by two types of cells, enterochromaffin (EC) cells and enteric serotonergic neurons in the myenteric plexus. The EC cells express tryptophan hydroxylase-1 (TPH1) to synthesize 5-HT and enteric serotonergic neurons express TPH2 to produce 5-HT.[19] 5-HT exerts its roles through engagement of 5-HT receptors. At least 14 members of 5-HT receptors have been identified up to date.[20] Most members of 5-HT receptors belong to the G-protein-coupled receptor (GPCR) superfamily, and only 5-HT3 receptor belongs to the ligand-gated ion channel. Different cell types harbor specific receptors to receive 5-HT stimulation. For instance, HTR2B is highly expressed in white adipocytes and hepatocytes, and promotes lipolysis and liver gluconeogenesis during fasting.[21] HTR3a is highly expressed in brown adipocytes and pancreatic β cells, and participates in systemic energy homeostasis, brown adipose tissue thermogenesis and glucose-stimulated insulin secretion.[22]

Intestinal epithelium is exposed to astounding numbers and diversity of microorganisms in the enteric cavity, collectively called gut microbiota.[23] The gut microbiota interacts with the host extensively and regulates various physiological and pathological processes. For example, the gut microbiota can regulate innate and adaptive immunological players, including epithelial cells, antigen-presenting cells, innate lymphoid cells and regulatory T cells.[24] The gut microbiota is also implicated in tumor initiation, progression and dissemination, as well as the response to cancer therapy.[25] In addition, germ-free (GF) mice show a reduced epithelial cell turnover rate owing to declined proliferation of intestinal epithelial cells and declined crypt-to-tip cellular migration.[26–28] A recent report showed that a lactic acid-producing bacterium plays a critical role in the ISC-mediated epithelial development.[29] Here, we investigated the regulatory role of microbiota–neuron crosstalk in ISC self-renewal, and found that gut microbiota metabolite valeric acid (VA) promotes 5-HT production in enteric serotonergic neurons. 5-HT signaling is required for the production of PGE2 in macrophages, which drives ISC self-renewal via engagement with its respective receptors Ep1/Ep4.

RESULTS

Microbiota is required for the maintenance and functions of ISCs

To determine the role of intestinal microbiota in ISC regulation, we kept $Lgr5^{GFP}$ reporter mice in SPF (specific pathogen free) and GF conditions. We observed that GF mice displayed decreased crypt depth and Ki67$^+$ ISC numbers (Fig. 1a). Fecal microbiota transplantation (FMT) is able to restore normal microbiota in GF mice.[30] We noticed that FMT into GF mice restored the crypt depth and ISC numbers (Fig. 1a). We then conducted organoid formation assays and found that microbiota was required for ISC function both in small intestines and colons (Fig. 1b). Mice treated with ampicillin, neomycin and vancomycin (ABX) can destroy microbiota. We observed that ABX-treated mice showed substantially impaired ISC numbers and organoid formation capacity (Supplementary information, Fig. S1a, b). Through lineage tracing, we observed that GF and ABX-treated mice showed dramatically decreased ISC numbers, whereas FMT treatment into GF mice was able to rescue the self-renewal capacity of ISCs (Fig. 1c, d; Supplementary information, Fig. S1c).

Given the critical role of ISCs in intestinal regeneration after radiation damage,[31] we then performed radiation damage followed by detection of intestinal regeneration. As expected, GF or ABX-treated mice showed dramatically impaired intestinal regeneration and repair ability (Fig. 1e; Supplementary information, Fig. S1d). These data indicate that microbiota plays a critical role in the maintenance and functions of ISCs.

Neurotransmitter 5-HT drives self-renewal of ISCs

We next wanted to explore the regulatory role of microbiota–neuron crosstalk in ISC self-renewal. To investigate whether intestinal nerve cells and neurotransmitters were involved in microbiota-mediated ISC self-renewal, we detected neurotransmitter concentrations of SPF and GF intestine tissues via mass spectrum-based metabolome analysis (Fig. 2a). We then chose top five differentially expressed neurotransmitters in GF mice and conducted in vivo blocking assays. We treated $Lgr5^{GFP}$ reporter mice with commercial neurotransmitter antagonists and counted GFP$^+$ ISC numbers in intestine tissues after 3 days. We found that the tryptophan hydroxylase inhibitor pCPA most significantly decreased the ratios of ISCs in both small intestines (SI) and colons (Fig. 2b). To further test 5-HT levels in the ISC niche, we isolated stem cell niche sections via laser capture microdissection (Supplementary information, Fig. S2a). We noticed that 5-HT levels were decreased in the ISC niche fraction from GF mice (Supplementary information, Fig. S2b). In addition, mice with pCPA treatment displayed decreased depth of crypts in small intestines and colons, and shortened villi (Fig. 2c). These observations were further confirmed by probing $Lgr5$ in situ hybridization (Fig. 2d). Moreover, pCPA treatment attenuated the intestinal regeneration ability after radiation damage (Fig. 2e). These data suggest that 5-HT plays a critical role in the maintenance of ISCs. To distinguish central and peripheral 5-HT synthesis, we used mesenteric artery injection (MAI) to enhance intestine-specific targeting with the inhibition of brain targeting.[32] We found that MAI treatment specifically blocked intestinal 5-HT synthesis but did not affect central 5-HT synthesis (Supplementary information, Fig. S2c). pCPA delivery by MAI obtained similar inhibitory effect on ISC maintenance, confirming that intestinal 5-HT is required for ISC self-renewal maintenance (Supplementary information, Fig. S2d).

In addition, we found that 5-HT injection largely restored 5-HT levels and ISC numbers in SI and colon tissues of GF mice (Supplementary information, Fig. S2e, f). Serotonin transporter (SERT) can recycle 5-HT to terminate its action, and $Sert$ deficient mice showed increased 5-HT levels.[33] We generated $Sert$-knockout (KO) mice (Supplementary information, Fig. S2g, h). $Sert$-deficient mice displayed increased 5-HT levels in ISC niche and decreased 5-HT levels in myenteric neurons (Supplementary information, Fig. S2i, j). We found that $Sert$-KO mice showed increased length of villi and crypts (Supplementary information, Fig. S2k). In addition, $Sert$-KO also increased ISC numbers in both small intestines and colons (Fig. 2f). To further perform lineage tracing, $LR^{lacZ};Sert^{-/-}$ mice were established by crossing $Sert$ KO mice with $Lgr5^{GFP-CreERT2}$ and $Rosa26^{lsl-lacZ}$ mice. We observed that $Sert$ deletion increased ISC numbers and intestinal renewal ability (Fig. 2g, h; Supplementary information, Fig. S2l). Altogether, 5-HT promotes the self-renewal maintenance of ISCs.

5-HT produced by enteric serotonergic neurons is required for ISC self-renewal

5-HT metabolism is a complicated process and numerous enzymes are involved in this process (Supplementary information, Fig. S3a). We examined expression levels of serotonin-metabolism-related genes and found $Tph1/2$ were downregulated in GF mice (Supplementary information, Fig. S3b). Within the gut, 5-HT is generated by EC cells and enteric serotonergic neurons of myenteric plexus. The EC cells contain tryptophan hydroxylase-1 (TPH1) responsible for biosynthesis of 5-HT, whereas enteric serotonergic neurons express TPH2 for 5-HT production.[34] To determine the source cells for 5-HT production, we generated $Tph1$-KO mice and obtained $Tph2$-KO mice (Supplementary information, Fig. S3c–e). We next detected 5-HT levels of total tissues and ISC niche fractions in $Tph1$-KO and $Tph2$-KO mice, and found a remarkable decrease of 5-HT in ISC niche in $Tph2$-KO mice (Supplementary information, Fig. S3f). We found that $Tph2$-KO mice displayed much shorter crypts and villi and reduced numbers of ISCs, whereas $Tph1$-KO mice showed normal ISCs compared to littermate wild-type (WT) mice (Fig. 3a; Supplementary information, Fig. S3g). These observations were further validated by staining for another ISC marker Olfm4 and
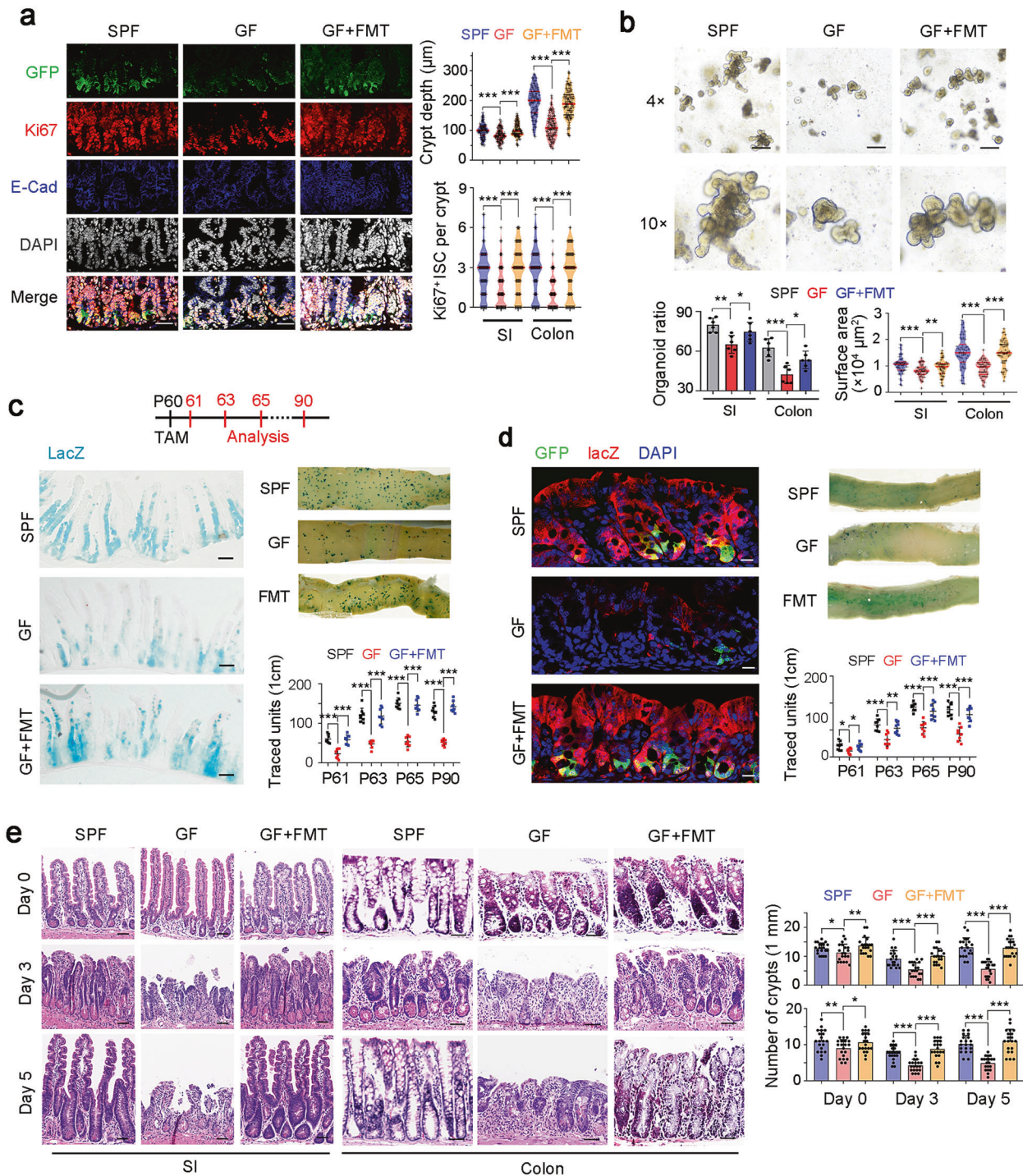
Fig. 1 Microbiota promotes ISC self-renewal. a SPF mouse, GF mice and GF mice with FMT were used for ISC detection. Typical images are shown in the left panels, and statistical results of crypts ($n = 100$) from five mice are in the right panel. Scale bars, 50 μm. 7-day FMT treatment was used for microbiota recovery, and proper conventionalization and depletion were confirmed by RT-PCR detection of 16 S rRNA. **b** Organoid formation of crypts obtained from SPF mice, GF mice and GF mice with FMT. Typical images are shown in the upper panels, and organoid formation ratios and the surface area of organoid are shown in the lower panels. **c** SPF, GF, and FMT into GF $Lgr5^{GFP-CreERT2}$; $Rosa26^{lsl-lacZ}$ (LR^{lacZ}) mice were treated with tamoxifen (TAM) for lineage tracing analysis. Mice ($n = 8$) were sacrificed at the indicated time points and typical sections of postnatal day 65 (P65) were shown. Numbers of traced crypt-villus units (blue plots) at indicated time points were shown. **d** LR^{lacZ} mice in SPF or GF states, and GF mice with FMT were treated with TAM for lineage tracing analysis. 5 days later, GFP and lacZ signals were detected by confocal microscopy. Representative images of 5 mice are shown. Scale bars, 20 μm. **e** SPF mice, GF mice and GF mice with FMT were treated with 10 Gy's radiation, and sacrificed at indicated time points. Intestinal tissues were collected for H&E staining (left panel) and numbers of intact crypts were shown in the right panel (means ± SD). 20 fields from five mice were taken for each group. Scale bars, 100 μm. *$P < 0.05$, **$P < 0.01$, ***$P < 0.001$, by unpaired one-tailed Student's t-test. Data were shown as means ± SD, and typical images are representative of three independent experiments.
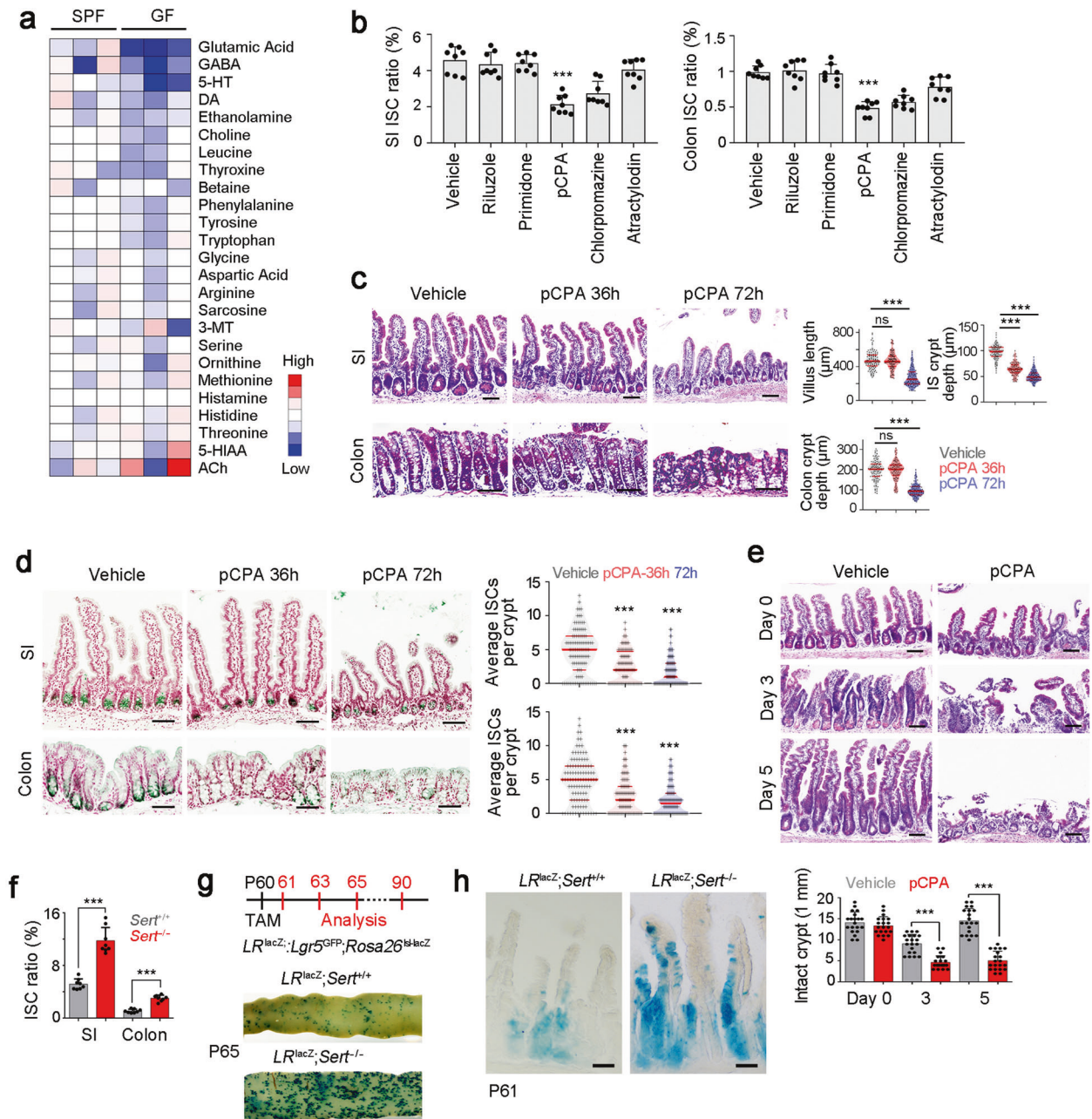
Fig. 2 5-HT drives self-renewal of ISCs. a The content of the indicated neurotransmitters in SPF and GF colon tissues were detected by mass spectrum, and normalized to the levels in SPF mice. SPF or GF mice ($n = 3$) were used for detection. GABA, γ-aminobutyric acid; 5-HT, 5-hydroxytryptamine; DA, dopamine; 3-MT, 3-methoxytyramine; 5-HIAA, 5-hydroxyindoleacetic acid; Ach, acetylcholine. **b** Two-month-old $Lgr5^{GFP}$ mice were treated with indicated neurotransmitters or neurotransmitter antagonists. Three days later, crypts of SI (left) and colon (right) were collected, and $Lgr5^{GFP+}$ ISCs were detected by FACS. Ratios of $Lgr5^{GFP+}$ ISCs in total crypt cells were shown as scatter diagram. Riluzole, glutamic acid antagonist; Primidone, GABA antagonist; pCPA, tryptophan hydroxylase inhibitor; Chlorpromazine, DA antagonist; Atractylodin, ethanolamine antagonist. $Lgr5^{GFP}$ mice ($n = 8$) for each group. **c** Two-month old mice were treated with 5-HT inhibitor pCPA for 36 h and 72 h, and representative H&E images of SI and colon were shown in left panel. 100 fields from five mice were observed and shown in right panel. 150 mg/kg pCPA was intraperitoneally injected. **d** $Lgr5$ in situ hybridization was performed in SI and colon tissues from pCPA-treated mice. Typical images were shown in left panel, and statistical results of 100 fields from five mice were shown in right panel. **e** pCPA-treated mice were treated with 10 Gy's radiation, and sacrificed at indicated time points. Intestinal tissues were collected for H&E staining (upper panel). Numbers of intact crypts were shown in lower panel (means ± SD). Five 2-month-old mice were used and 20 fields were taken for each group. 150 mg/kg pCPA was intraperitoneally injected. **f** $Sert$ KO SI and colon crypts were collected for ISC detection by FACS. $Lgr5^{GFP}$; $Sert^{+/+}$ ($Sert^{+/+}$) or $Lgr5^{GFP}$; $Sert^{-/-}$ ($Sert^{-/-}$) mice ($n = 8$) were used and the ratios of $Lgr5^{GFP+}$ ISCs were shown. **g** LR^{lacZ} mice were crossed with $Sert^{-/-}$ mice, followed by administration of TAM for lineage tracing analysis through intestinal whole-mount staining for β-gal. 200 μL TAM in sunflower oil (10 μg/μL) was intraperitoneally injected. 7 mice were sacrificed at indicated time points and typical sections of P65 were shown. **h** LR^{lacZ};$Sert^{-/-}$ mice were used for lineage tracing analysis, and intestinal tissues were stained for lacZ. $n = 7$ mice per group. For **c–e**, scale bars, 100 μm. *$P < 0.05$; **$P < 0.01$; ***$P < 0.001$; ns, not significant; statistics was performed by unpaired one-tailed Student's t-test. At least three independent repeats were performed for each experiment and the representative results were shown.
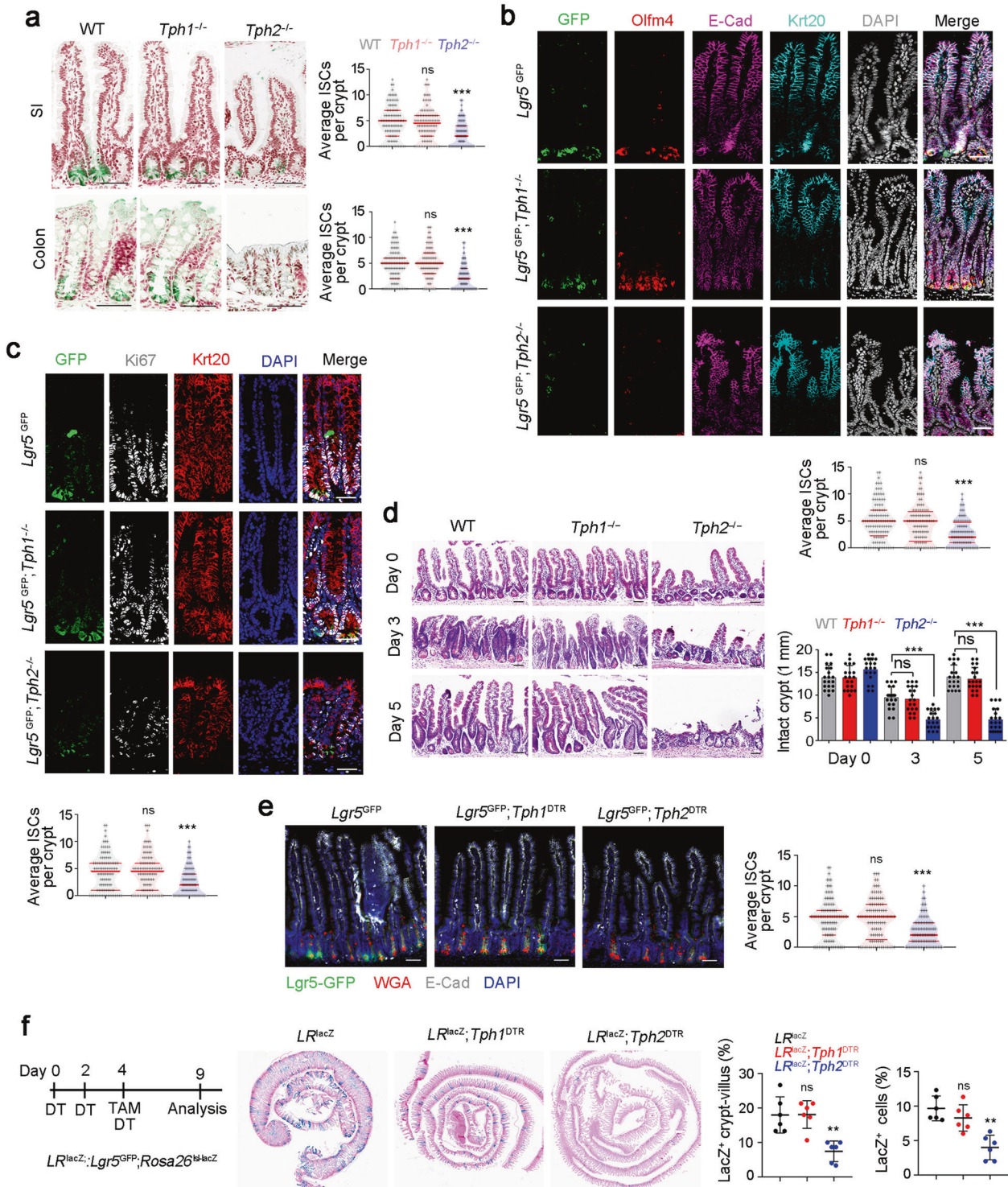
Fig. 3 5-HT generated by enteric serotonergic neurons contributes to ISC self-renewal. a *Lgr5* in situ hybridization was performed in SI and colon tissues from *Tph1-* and *Tph2*-KO mice. Typical image were shown in left panel, and 100 fields from five mice were observed and shown in right panel. Scale bars, 100 μm. **b**, **c** *Lgr5^GFP^;Tph1^−/−^* mice and *Lgr5^GFP^;Tph2^−/−^* mice were sacrificed on P60 and intestine tissues were collected for immunofluorescence staining by indicated antibodies. Typical images of small intestine (**b**) and large intestine (**c**) are shown. 100 fields from five mice were observed and calculated. Scale bars, 50 μm. **d** *Tph1* and *Tph2* KO mice were treated with 10 Gy's radiation, and sacrificed at indicated time points. Intestinal tissues were collected for H&E staining (upper panel) and numbers of intact crypts were shown in lower panel (means ± SD). 20 fields from five mice were taken for each group. Scale bars, 100 μm. **e** Fluorescence staining of intestinal tissue from 2-month-old *Lgr5^GFP^*, *Lgr5^GFP^*; *Tph1^DTR^* and *Lgr5^GFP^;Tph2^DTR^* mice 6 days after the first diphtheria toxin (DT) treatment. 100 ng/mouse DT treatments were performed on day 0 and day 3. 100 fields from five mice were observed. Scale bars, 50 μm. **f** *LR^lacZ^;Tph1^DTR^* and *LR^lacZ^;Tph2^DTR^* mice were treated with 100 ng/mouse DT every 3 days, and used for lineage tracing analysis, and intestinal tissues were stained for lacZ observation. 6 mice were used. *$P < 0.05$, **$P < 0.01$, ***$P < 0.001$ by unpaired one-tailed Student's *t*-test. *$P < 0.05$, **$P < 0.01$, ***$P < 0.001$ by unpaired one-tailed Student's *t*-test; ns, not significant. At least three independent repeats were performed for each experiment and the representative results were shown.

proliferation marker Ki67 antigen (Fig. 3b, c). Moreover, *Tph2* KO mice also showed impaired intestinal regeneration post-radiation damage (Fig. 3d). Of note, 5-HT was an essential factor for ISC function in $Tph2^{-/-}$ mice via 5-HT injection assay (Supplementary information, Fig. S3h). Additionally, peripheral TPH2$^+$ cells were required for ISC maintenance through mesenteric artery injection of 5-HT to *Tph2*-KO mice (Supplementary information, Fig. S3i–k).

To further verify the role of EC cells and enteric serotonergic neurons in ISC self-renewal, we generated $Tph1^{DTR}$ and $Tph2^{DTR}$ mice through CRISPR/Cas9 approaches, in which EC cells and enteric serotonergic neurons will be depleted upon diphtheria toxin (DT) treatment (Supplementary information, Fig. S3l–n). As expected, decreased ISC numbers and impaired ISC function could be observed in DT-treated $Tph2^{DTR}$ mice, whereas DT-treated $Tph1^{DTR}$ mice had normal ISC number and normal function compared to $Lgr5^{GFP}$ mice (Fig. 3e, f). 5-HT was an essential factor for ISC function in DT-treated $Tph2^{DTR}$ mice (Supplementary information, Fig. S3o). Moreover, depletion of Tph2$^+$ enteric serotonergic neurons caused impaired ISC maintenance and decreased ISC gene expression (Supplementary information, Fig. S3p–r). These observations confirm that enteric serotonergic neurons play a critical role in ISC self-renewal and intestinal regeneration. Taken together, enteric serotonergic neurons are required for ISC self-renewal and intestinal regeneration.

Microbiota metabolite VA initiates *Tph2* expression by inhibiting recruitment of the NuRD complex

In many cases, microbiota secretes metabolites to participate in the regulation of biological processes.[35] We then used absorbable metabolites to treat GF mice and examined *Tph2* expression levels in intestinal tissues.[36] Of these metabolites we examined, VA could dramatically promote *Thp2* expression in GF mice, while other metabolites we used had no such effect (Fig. 4a; Supplementary information, Table S1). We treated $Lgr5^{GFP}$ mice with other short chain fatty acids (SCFAs), and found only VA promoted expression of *Tph2* and ISC signature genes (Supplementary information, Fig. S4a). The observation that *Tph2* expression was enhanced by VA was further validated by immunoblotting (Fig. 4b). In addition, VA could promote expression of ISC proliferation-related genes in GF intestine (Fig. 4b). Moreover, VA treatment was able to enhance 5-HT generation in GF myenteric plexus, similar with FMT treatment (Fig. 4c; Supplementary information, Fig. S4b). Of note, FMT and VA treatment could augment ISC-related gene expression and restore ISC numbers, but failed to do so in the *Tph2*-deleted mice, suggesting FMT and VA promoted ISC self-renewal in a TPH2-dependent manner (Fig. 4d, e). A recent report showed that *Megasphaera massiliensis* is a source to produce VA.[37] We then transferred *Megasphaera massiliensis* to SPF or GF mice via intragastric administration. We found that *Megasphaera massiliensis* administration increased VA levels in intestines of GF and SPF mice (Supplementary information, Fig. S4c, d), consequently promoted expression of ISC signature genes and proliferation genes (Supplementary information, Fig. S4e). Neuron depletion in $Tph2^{DTR}$ mice confirmed the essential role of serotonergic neurons in the microbiota and VA-mediated ISC maintenance (Fig. 4f, g). Similarly, ABX inhibited ISC maintenance in a TPH2-dependent manner (Supplementary information, Fig. S4f). Collectively, VA secreted by microbiota promotes *Tph2* expression and 5-HT-mediated ISC self-renewal.

To further explore the molecular mechanism of microbiota-mediated *Tph2* expression, we isolated myenteric plexus cells from GF mice and SPF mice, and examined chromatin accessibility of *Tph2* promoter by DNase protection assay. We found that the −3600~−3400 region of *Tph2* promoter was resistant to DNase digestion in GF mice, suggesting the *Tph2* promoter is suppressed in GF mice (Supplementary information, Fig. S4g). The activation of *Tph2* promoter by VA was validated by luciferase assay

(Supplementary information, Fig. S4h). HDAC1, HDAC2 and MBD3, which are main components of the NuRD complex that inhibits gene transcription,[38] were identified as protein candidates for binding *Tph2* promoter in GF cells through CAPTURE assay (Capture of Chromatin Interactions by Biotinylated dCas9)[39] (Fig. 4h; Supplementary information, Fig. S4i). Enhanced interaction of *Tph2* promoter with these three components was confirmed by Western blot. However, FMT and VA treatment blocked the interaction of NuRD complex with *Tph2* promoter (Fig. 4i). These observations were further confirmed by chromatin immunoprecipitation (ChIP) and fluorescence in situ hybridization (FISH) assays (Fig. 4j, k; Supplementary information, Fig. S4j). These data suggest that FMT and VA treatment can reduce the enrichment of the NuRD complex onto *Tph2* promoter. H3K5ac and H3K9ac are two histone H3 modifications that are removed by HDAC1/2.[40] H3K4me3 is an active marker for gene transcription activation.[41] We found that FMT and VA treatment enriched H3K5ac, H3K9ac and H3K4me3 onto *Tph2* promoter region (Fig. 4l). To further examine the direct or indirect role of VA in 5-TH production and release, we established in vitro culture system of myenteric plexus neurons.[42] We observed that VA treatment increased *Tph2* expression (Supplementary information, Fig. S4k, l) and promoted 5-HT levels (Supplementary information, Fig. S4m). In addition, blocking the NuRD complex activity impaired VA-mediated 5-HT production, further confirming that VA directly regulates *Tph2* expression through the NuRD complex (Supplementary information, Fig. S4k–m). Altogether, VA inhibits enrichment of the NuRD complex onto *Tph2* promoter to initiate its expression.

5-HT activates *Ptges* expression in macrophages

We next explored the molecular mechanism of 5-HT in ISC self-renewal. First, we established organoid formation assay with ISC, crypt or ISC plus CD45$^+$ cells, and found 5-HT mainly activated ISC self-renewal through CD45$^+$ cells (Fig. 5a, b; Supplementary information, Fig. S5a, b). Among top10 downregulated genes in *Tph2*-deficient CD45$^+$ cells, *Ptges*, a critical gene for PGE2 expression, was required for CD45$^+$ cells-dependent ISC self-renewal (Fig. 5c, d). Of note, *Ptges*-KO mice showed decreased numbers of ISCs in both small intestines and colons (Fig. 5e; Supplementary information, Fig. S5c, d). Moreover, pCPA treatment impaired ISC function in WT mice, but not in *Ptges*-KO mice, indicating an essential role of *Ptges* in 5-HT-mediated ISC self-renewal and function (Fig. 5e). A previous study showed that fibroblasts is a key PGE2 producer in the intestinal stem cell niche.[43] We then treated recipient mice with 10 Gy's irradiation, and performed bone marrow transplantation to compare differential functions of stromal and myeloid PGE2 (Supplementary information, Fig. S5e). In SPF condition, WT bone marrow transplant into *Ptges*-KO mice promoted expression of ISC signature genes and proliferation genes, and non-myeloid cells (stromal cells) also participated in ISC activation. In contrast, myeloid cells showed impaired role in ISC activation and stromal cells played a predominant role in GF condition (Supplementary information, Fig. S5f).

Ptges was widely expressed in CD45$^+$ immune cells, and especially macrophages, which exhibited 5-HT dependent *Ptges* expression (Fig. 5f). Indeed, macrophage depletion largely decreased ISC numbers in both small intestines and colons (Fig. 5g). Adoptive transfer of WT macrophages, but not $Ptges^{-/-}$ macrophages, was able to rescue ISC numbers in *Tph2*-depleted mice (Fig. 5h), indicating that 5-HT exerts its role in ISC self-renewal mainly through PGE2 in macrophages. Similarly, in organoid formation assays, 5-HT-promoted ISC self-renewal required PGE2$^+$ macrophage activation (Fig. 5i). We next cultured myenteric plexus neurons from WT and *Tph2*-KO mice with or without macrophages for organoid formation assay.[42] We observed that *Tph2*-KO myenteric plexus neurons impaired
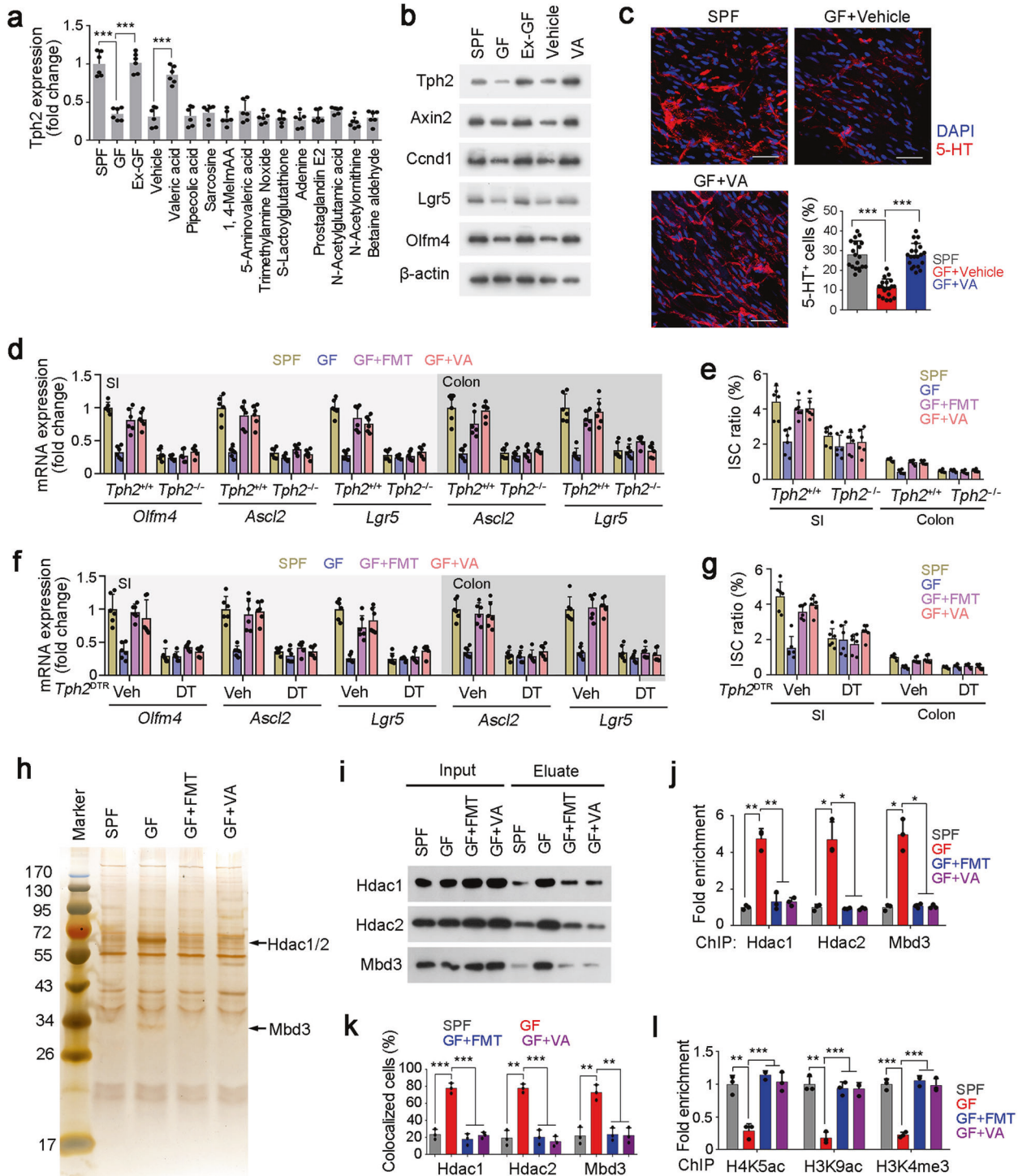
organoid formation in a macrophage-dependent manner (Supplementary information, Fig. S5g).

We also examined the role of macrophages in 5-HT-mediated ISC maintenance. We noticed that none of microbiota, VA or 5-HT affected ISC numbers in macrophage-depleted mice (Fig. 5j, k; Supplementary information, Fig. S5h, i). Moreover, macrophage-depleted mice showed impaired intestinal regeneration post-radiation damage, and microbiota-VA-5-HT axis failed to regulate the intestinal regeneration upon macrophage depletion (Fig. 5l). These results indicate that intestinal macrophages are required for the 5-HT-mediated ISC maintenance.

5-HT promotes PEG2 expression in PGE2$^+$ macrophages via engagement with its receptors HTR2A and HTR3A

5-HT exerts its role through its cognate receptors, so we next detected the expression patterns of 5-HT receptors on macrophages. We silenced each receptor in macrophages and detected the role of 5-HT in *Ptges* expression. We noticed that *Htr2a* or *Htr3a* knockdown decreased *Ptges* expression, whereas knockdown of other 5-HT receptors had no significant inhibition (Fig. 6a). Indeed, *Htr2a* and *Htr3a* were highly expressed in macrophages (Fig. 6b). Moreover, blockade of HTR2A and HTR3A with their inhibitors Ketanserin and Tropisetron suppressed 5-HT-

Fig. 4 **VA reduces enrichment of the NuRD complex onto *Thp2* promoter to initiate its expression. a** GF mice were treaded with indicated metabolites, and *Thp2* in intestine tissues was detected by RT-PCR. SPF and Ex-GF mice were used for positive controls. 6 mice were treated with metabolites daily for 5 days per group. Ex-GF mice denote conventional mice which were exited from GF condition. **b** Total intestine tissues from treated mice were lyzed for western blot. β-actin was used as a loading control. 3 mice were detected with similar results. VA, valeric acid. **c** Myenteric plexus was isolated from treated mice, and 5-HT was detected by confocal microscopy. Typical images and 5-HT$^+$ ratios were shown. 20 fields from five mice were taken for each group. Blue, DAPI; Red, 5-HT. Scale bars, 50 μm. **d** SI and colon tissues were isolated from treated *Tph2* KO and control mice were used for RT-PCR analysis. ISC marker genes (*Olfm4, Ascl2, Lgr5*) were detected and normalized to the levels of SPF mice. 6 mice were detected per group. **e** SI and colon crypts were obtained from treated *Tph2*-KO and control mice, and ISCs were detected by FACS. 6 mice per group. **f, g** *Tph2*^{DTR} mice were treated with DT for serotonergic neuron depletion, followed by ISC markers and ISC ratio detection as in **d, e**. **h** Silver staining of eluate from CAPTURE assay using SPF-, GF- or VA-treated myenteric plexus cells. Increased bands in GF cells were identified as HDAC1, HDAC2 and MBD3. **i** The interaction of *Tph2* promoter with HDAC1, HDAC2, and MBD3 in indicated myenteric plexus was detected by CAPTURE assay and Western blot. **j** Indicated myenteric plexus cells were obtained for ChIP assay against HDAC1, HDAC2, and MBD3. Enrichment of *Thp2* promoter (−3600~−3400 region) was examined by RT-PCR. **k** Enteric serotonergic neurons were sorted by TPH2 and confirmed by 5-HT staining, followed by FISH for *Tph2* promoter detection and immunofluorescence staining for HDAC1. Ratios of co-localized cells in enteric serotonergic neurons isolated from indicated treatment mice were shown. 3 mice were used per panel, and 100 cells were observed per mouse. **l** H4K5ac, H3K9ac, and H3K4me3 modifications of *Thp2* promoter were detected by ChIP assay. −3600~−3400 region of *Thp2* promoter were detected by RT-PCR. *$P < 0.05$; **$P < 0.01$; ***$P < 0.001$; ns, not significant. Statistics was performed by unpaired one-tailed Student's *t*-test. At least three independent repeats were performed for each experiment and the representative results were shown.

dependent PGE2 production (Fig. 6c). We then generated *Htr2a* and *Htr3a* KO mice, and established double KO (DKO) mice by crossing these KO mice (Supplementary information, Fig. S6a–d). Decreased PGE2 release was observed in *Htr2a* and *Htr3a* KO macrophages (Fig. 6d). These data suggest that HTR2A and HTR3A are required for 5-HT-dependent PGE2 production. More importantly, *Htr2a* and *Htr3a* KO mice showed decreased numbers of ISCs, indicating the essential role of Htr2a and Htr3a in ISC maintenance (Fig. 6e).

We then examined PGE2 function in ISC self-renewal. PGE2 treatment increased ISC numbers, whereas PGE2 inhibitor indomethacin treatment decreased ISC numbers (Fig. 6f, g). In addition, PGE2 treatment promoted organoid formation of ISCs (Fig. 6h), suggesting a critical role of PGE2 in ISC self-renewal. Intriguingly, we found that PGE2 was enriched in a subpopulation of macrophages, and the ratios of PGE2$^+$ macrophages were decreased in GF mice, whereas FMT and VA treatment restored the ratios of PGE2$^+$ macrophages (Fig. 6i; Supplementary information, Fig. S6e, f). We used FACS to analyze CD45.1 cell numbers and their intracellular levels of PGE2 in transfer assays. We observed that macrophages mainly distributed in the host SI (Supplementary information, Fig. S6g). PGE2 levels in transferred macrophages were comparable to WT mice when ISCs were detected two days post transfer (Supplementary information, Fig. S6h, i).

Previous reports revealed that surface markers CX3CR1 and P2RX4 are required for PGE2 production in macrophages.[44,45] We observed that PGE2$^+$ cells highly expressed CX3CR1 and P2RX4 (Supplementary information, Fig. S7a). Moreover, CX3CR1^{hi} P2RX4$^+$ cells were able to generate PGE2, but not CX3CR1^{int}, CX3XR1^{neg}, or CX3CR1^{hi} P2RX4$^-$ cells (Supplementary information, Fig. S7b, c), We concluded that CX3CR1^{hi} P2RX4$^+$ cells were related to the PGE2$^+$ macrophage subset. We also confirmed that CX3CR1^{hi}P2RX4$^+$ cells were regulated by microbiota and metabolite VA (Supplementary information, Fig. S7d, e). It has been reported that intestinal macrophages are either from embryonic precursors or adult bone marrow-derived monocytes.[46] Based on our bone marrow transplant assay, we found that PGE2$^+$ bone marrow could generate PGE2$^+$ macrophages that maintained the self-renewal of ISCs (Supplementary information, Fig. S5e, f), suggesting that PGE2$^+$ macrophages are bone marrow-derived. A previous report showed that intestinal macrophages contain two groups, lamina propria macrophages (LpMs) and muscularis macrophages (MMs).[47] We noticed that PGE2$^+$ macrophages both distributed in muscularis and lamina propria (new Supplementary information, Fig. S7f, g).

We then isolated PGE2$^+$ and PGE2$^-$ macrophages for adoptive transfer. We found that more PGE2$^+$ macrophages distributed in ISC niche than PGE2$^-$ macrophages (Fig. 6j; Supplementary information, Fig. S7h). In myenteric plexus, PGE2$^+$ macrophages

were mainly localized near zones with high 5-HT content (Supplementary information, Fig. S7i). We also simultaneously showed the presence of enteric serotonergic neurons, PGE2$^+$ macrophages and ISCs, and confirmed that PGE2$^+$ macrophages existed in both myenteric plexus (near serotonergic neurons) and lamina propria (near ISCs) (Supplementary information, Fig. S7j). In addition, adoptive transfer of PGE2$^+$ macrophages dramatically restored ISC ratios in GF mice and serotonergic neuron-depleted mice (Fig. 6k). These results suggest that PGE2$^+$ macrophages are involved in the ISC self-renewal maintenance. Finally, we observed that 5-HT activated NF-kB signaling pathway to initiate *Ptges* expression (Supplementary information, Fig. S7k–n). Altogether, 5-HT activates PGE2 production through its cognate receptors HTR2A and HTR3A on macrophages.

PGE2 promotes ISC self-renewal through Wnt/β-catenin signaling

The mechanism of PGE2 in ISC self-renewal is not clear. We silenced all four PGE2 receptors in our in vitro organoid formation assays. We found that knockdown of *Ep1* or *Ep4* remarkably suppressed organoid formation (Fig. 7a). We next generated EP1 and EP4 knockout mice, and these mice displayed shorter crypts and villi, and DKO mice showed much shorter crypts and villi than each single KO mice (Fig. 7b; Supplementary information, Fig. S8a–d). Expectedly, *Ep1*, *Ep4* KO mice and DKO mice showed decreased ISC numbers (Fig. 7c, d). These results indicate that PGE2 signaling mediated by EP1 and EP4 is required for the ISC maintenance. In addition, DKO mice displayed impaired intestinal regeneration after radiation damage (Fig. 7e). Reduced ISC stemness was further validated by lineage tracing assays (Fig. 7f). To further determine cell-autonomous act of EP1 and EP4 in ISC regulation, we isolated WT, *Ep1*$^{−/−}$, *Ep4*$^{−/−}$ and DKO ISCs, supplemented with dmPGE2 or macrophages plus 5-HT for organoid formation. We found both EP1 and EP4 function in an ISC-intrinsic manner (Supplementary information, Fig. S8e). We then transferred WT macrophages to *Ep1*$^{−/−}$ and *Ep4*$^{−/−}$ mice and found WT macrophages could not rescue ISC phenotype in these two KO mice (Supplementary information, Fig. S8f). Collectively, PGE2 signaling is initiated by engagement with its receptors EP1 and EP4 to maintain ISC stemness.

Considering the crosstalk between PGE2 and Wnt/β-catenin signaling, we next detected Wnt/β-catenin activation. We noticed that DKO ISCs showed reduced inhibition o Wnt/β-catenin signaling activation (Fig. 7g; Supplementary information, Fig. S8g, h). In addition, we crossed DKO mice with *Axin2*^{lacZ} mice and found that DKO ISCs displayed impaired Wnt/β-catenin activation (Fig. 7h). These data indicate that PGE2 signaling promotes Wnt/β-catenin signaling activation. Taken together, PGE2 promotes ISC self-renewal through Wnt/β-catenin signaling.
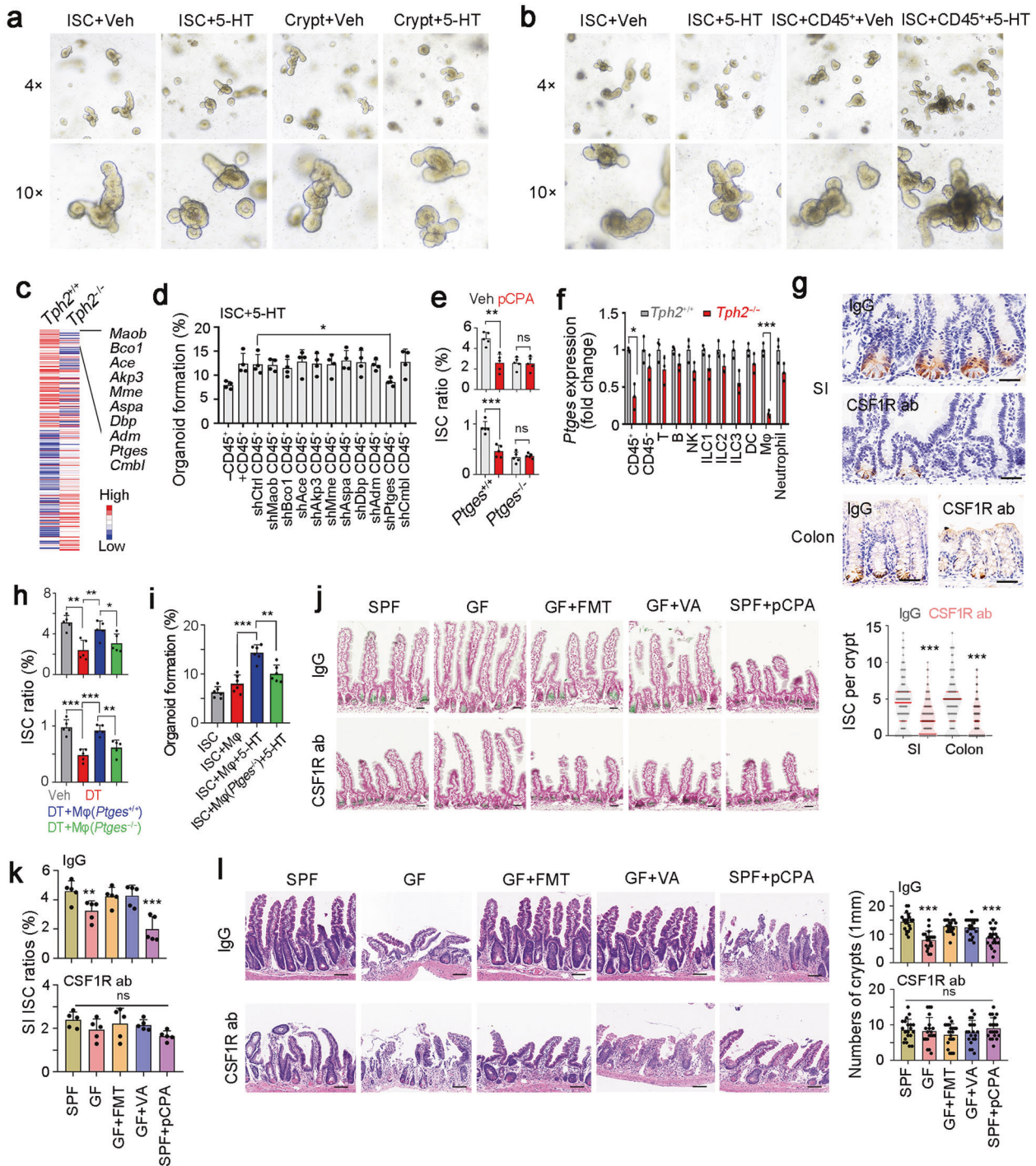
DISCUSSION

Under homeostatic conditions, the intestinal epithelium harbors remarkable self-renewal capacity that is driven by ISCs residing within specialized niches at the crypt base.[48] The self-renewal of ISCs is under precise regulation by various intracellular and extracellular signals. In this study, we showed that neurotransmitter 5-HT and PGE2 are required for the self-renewal maintenance of ISCs and intestinal regeneration. PGE2+ macrophages serve as crypt niche cells, which promote Wnt/β-catenin signaling in ISCs through engagement with PGE2 receptors EP1/EP4. VA produced by gut microbiota promotes *Tph2* expression in the enteric serotonergic neurons through suppression of recruitment of the NuRD complex. Our work reveals the crosstalk between microbiota, enteric neurons, immune cells and intestinal stem cells, adding a new layer for intestinal homostastasis regulation. Of note, treatment with FMT or VA does not completely restore PGE2+ macrophage frequencies in GF mice, suggesting that there might be an alternative mechanism that contributes to the phenotype. The precise mechanisms of development and cell fate determination of PGE2+ macrophage subset need to be further investigated.

The intestinal 5-HT is generated by two types of cells, EC cells and enteric serotonergic neurons of the myenteric plexus, respectively being synthesized by rate-limiting enzymes TPH1

Fig. 5 5-HT functions through macrophages. a, b Organoid formation of ISC and crypt (**a**), or ISCs co-cultured with CD45$^+$ cells (**b**). Organoid formation medium was supplemented with or without 5 μM 5-HT. 4 mice were used for organoid formation. **c** Heat map of *Tph2*-KO and control CD45$^+$ cells, with top10 low expressed genes in *Tph2* knockout cells listed in right. Red, high expression; Blue, low expression. **d** Organoid formation ratios of ISCs co-cultured with CD45$^+$ immune cells in which indicated genes were silenced individually, supplemented with 5 μM 5-HT. Results are from 4 independent experiments. **e** ISC ratios of *Ptges*$^{+/+}$ and *Ptges*$^{-/-}$ mice, which were treated with 150 mg/kg pCPA 3 days before ISC detection. 5 mice were used for ISC detection. **f** RT-PCR analysis for *Ptges* expression in indicated cells isolated from *Tph2*$^{+/+}$ and *Tph2*$^{-/-}$ mice. 3 *Tph2*$^{+/+}$ and *Tph2*$^{-/-}$ mice were used. **g** *Lgr5* in situ hybridization in SI and colon tissues of macrophage-depleted mice, which were intraperitoneally injected with CSF1R ab (antibody, 10 mg/kg). 100 fields from five mice were taken for each group. Scale bars, 50 μm. **h** FACS detection for ISC ratios in SI and colon crypts from indicated treated mice. For each group, 5 *Tph2*^{DTR} mice were treated with 100 ng DT every 3 days (twice), and adoptively transferred with 2×10^6 macrophage cells (Mφ). Mφ were activated by 5 μM 5-HT for 8 h and ISCs were detected 2 days after Mφ adoptive transfer. **i** Organoid formation of ISCs, co-cultured with WT or *Ptges*-KO macrophages and 5 μM 5-HT. $n = 6$ mice were used for each group. **j** *Lgr5* in situ hybridization was performed in small intestine from the indicated mice. Scale bars, 50 μm. **k** CSF1R antibody (ab) treated and control small intestine crypts were collected for ISC detection by FACS. 5 mice were used per group and ratios of ISCs were shown. **l** The indicated mice were treated with 10 Gy's radiation, and sacrificed at 5 days after radiation. Intestinal tissues were collected for H&E staining (upper panel) and numbers of intact crypts were shown in lower panel (means ± SD). $n = 20$ fields from five mice were taken for each group. Scale bars, 100 μm. *$P < 0.05$, **$P < 0.01$, ***$P < 0.001$ by unpaired one-tailed Student's *t*-test. At least three independent repeats were performed for each experiment and the representative results were shown.

and TPH2.[34] The 5-HT generated by the EC cells overflows to gastrointestinal lumen and blood. Overflowing 5-HT from the EC cells is taken up and concentrated in platelets as a sole source of blood 5-HT. It has been reported that the 5-HT generated by the enteric serotonergic neurons mediates fast and slow excitatory neurotransmission and regulates gastrointestinal motility.[49] Gross's work showed that *Tph2*$^{-/-}$ (but not *Tph1*$^{-/-}$) mice display decreased crypt depth and impaired crypt proliferation, and *Sert*$^{-/-}$ mice show an opposite effect.[33] To our knowledge, little is known whether and how the neuronal 5-HT and Tph2$^+$ enteric serotonergic neurons regulate ISC function. In our study, we identified 5-HT as a novel niche factor and Tph2$^+$ neurons as a novel niche cell subpopulation to regulate ISCs, and also provided a full mechanism from *Tph2* expression by valeric acid to the ISC function mediated by neuronal 5-HT.

5-HT exerts its functions through engagement with 5-HT receptors, including 13 distinct heptahelical GPCRs and one ligand-gated ion channel.[20] 5-HT and its receptors are identified to exist in both the central and peripheral nervous system, and they are also present in non-neuronal tissues such as gut, cardiovascular system and blood. Here, we found that *Htr2a* and *Htr3a* are highly expressed on macrophages and these receptors mediate the effect of 5-HT signaling on PGE2 production. Upon 5-HT engagement, these receptors activate *Ptges* expression, which induces PGE2 production. PGE2 further promotes Wnt/β-catenin activation and ISC self-renewal through EP1 and EP4. As one of the most important pathways in stem cells, Wnt/β-catenin is modulated precisely. We have identified several modulators in Wnt regulation,[50–52] and here we have revealed 5-HT-PGE2-Wnt axis in ISC self-renewal. A recent work showed that a subset of PTGER4-expressing intestinal macrophages (PTGER4$^+$ intestinal macrophages) is a driver of epithelial regeneration during recovery upon intestinal inflammation, serving as niche cells of ISCs, but macrophage specific PTGER4 deficiency has no impact on gut homoeostasis.[53] Here, we show that *Ep1* and *Ep4* are highly expressed on ISCs and *Ep1/Ep4* DKO impairs ISC self-renewal maintenance. We conclude that EP1 and EP4 function in an ISC-intrinsic manner.

Intestinal macrophages play critical roles in intestinal development, homeostasis, regeneration, aging, pathogen infection as well as inflammation.[46,54] Intestinal macrophages are a kind of tissue resident macrophages, and their functions are also finely regulated by various tissue factors. Increasing evidence indicates the critical role of macrophages in intestinal stem cells. CSF1R blockade causes a decrease of Lgr5$^+$ ISCs and aberrant differentiation of intestinal epithelial cell lineages.[55] AhR ablation in intestinal macrophages also disturbs intestinal epithelium development.[56] Macrophages secrete hepatocyte growth factor to promote ISC self-renewal and differentiation.[57] Here we reveal a novel mechanism of intestinal macrophages in

ISC self-renewal. Intestinal macrophages serve as signal transmitting cells in a neuro-immune-stem cell regulatory circuit, and modulate ISC self-renewal by upstream enteric serotonergic neurons. Intestinal macrophages express *Htr2a* and *Htr3a*, which are required for the initiation of 5-HT signaling from enteric serotonergic neurons. Engagement of 5-HT with its receptors Htr2a/3a in intestinal macrophages promote *Ptges* expression and PGE2 release, which drives the self-renewal of ISCs via Wnt/β-catenin pathway. Besides intestinal macrophages, some 5-HT receptors are also expressed in intestinal epithelial cells,[58] whose exact roles in the self-renewal of ISCs still need to be further investigated.

Gut microbiota plays critical roles in host health and disease, whose modulations mainly depend on direct stimulation by bacterial cell components and the effects of bacterial metabolites.[59] The bacterial cell components affect the physiological and pathological functions of the immune system via the direct stimulation of Toll-like receptors (TLRs) expressed by dendritic cells and colonocytes in the colonic mucosa.[60] Only a few of bacterial metabolites such as short-chain fatty acids (SCFA) have been defined,[61] most of them are not well known yet. Here we demonstrate only VA drives expression of *Tph2* and ISC signature genes. A recent report showed that many bacterial metabolites can be absorbed by colonocytes and into somatic blood,[36] indicating the critical roles of bacterial metabolites in the regulation of host health and disease. Kaiko et al. reported that many bacterial metabolites suppress ISC self-renewal in the organoid formation assay.[62] Here we showed that the gut microbiota and metabolite VA are required for ISC self-renewal and intestinal regeneration. Moreover, VA can inhibit enrichment of the NuRD complex onto *Tph2* promoter, thus initiating *Tph2* expression, which promotes 5-HT production in enteric serotonergic neurons. In our study, we demonstrate that the bacterial metabolite VA can induce ISC self-renewal by an in vivo lineage tracing assay. The differences between Kaiko et al. and our findings suggest that specific bacterial metabolites may have different roles in the regulation of intestinal homeostasis and regeneration. Our work adds a new layer of ISC regulation by niche enteric nervous system, enteric immune cells and gut microbiota.

Different segments of intestines and colons differ in microbe levels. In this study, we focus on the ileum and colon, which show similar phenotypes. We show that injected *Megasphaera massiliensis* was distributed in both ileum and colon section. As for the segment distributions of other microbes, it needs to be further investigated. The link between gut microbiota and intestinal epithelium homeostasis is a fascinating field, and increasing studies reveal "microbiota–epithelium" crosstalks such as "fungal metabolite–macrophage–epithelium integrity" axis[63] and "lactic acid-producing bacteria–lactic acid–intestinal stem cell–epithelial development" axis.[29] Lee et al revealed that lactic acid-producing bacteria
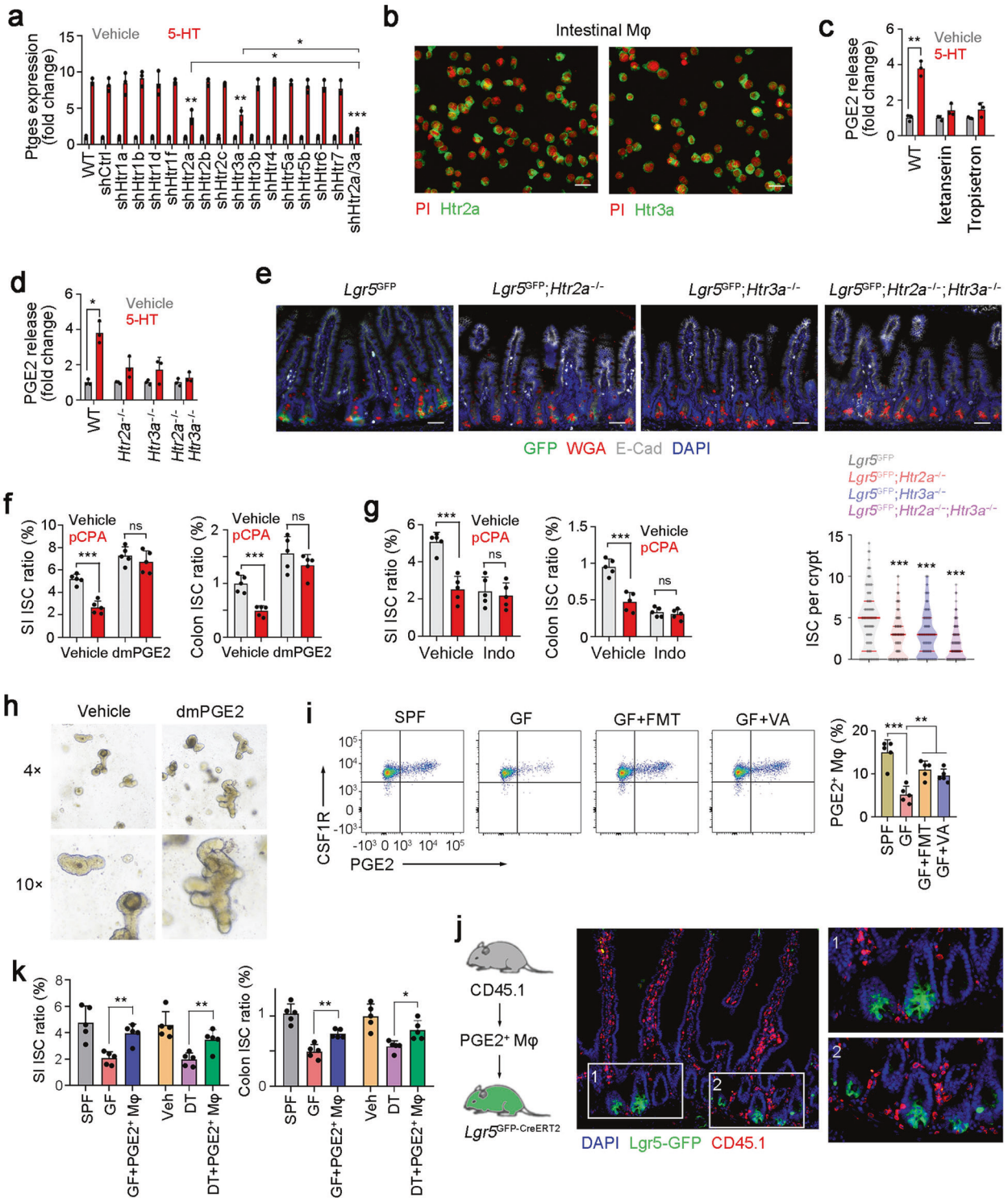
promote the ISC-mediated epithelial development via lactic acid receptor GPR81, which is expressed on Paneth and stromal cells.[29] However, little is known about the crosstalk between microbiota and intestinal nerve cells, and the effect of "microbiota–nerve" crosstalk on the stemness regulation of ISCs. Herein, we reveal novel niche factors (including microbiota metabolite VA and neurotransmitter 5-HT) and niche cells (enteric serotonergic neurons, PGE2$^+$ macrophages) for ISC self-renewal maintenance, which provides an additional layer for ISC regulation.

MATERIALS AND METHODS

Antibodies and reagents

Anti-Olfm4 (#14369), anti-EPCAM (#14452) and anti-E-Cadherin (#8437S) antibodies were from Cell Signaling Technology. Anti-GFP (#ab183735), anti-Ki67 (#ab15580), and anti-Digoxin (#ab51949) antibodies were obtained from Abcam. Anti-WGA (#GTX01500) antibody was purchased from GeneTex. Anti-β-catenin (#610154) antibody was obtained from BD Biosciences. Anti-Krt20 (#17329-1-AP) antibody was purchased from Proteintech. Streptavidin-conjugated CD45 antibody (#AC12-0147-22) was from Abcore. Biotin-conjugated PGE2 antibody (#EU2554) was from Fine Biotech. Anti-PGE2

Fig. 6 5-HT promotes PGE2 expression with engagement with its receptors HTR2A and HTR3A. a RT-PCR detection of *Ptges* expression levels in 5-HT treated intestinal macrophages, in which the indicated 5-HT receptors were silenced individually. 2×10^5 indicated silenced intestinal macrophages were treated with 5 μM 5-HT for 8 h, and *Ptges* expression was detected 24 h later. Results are from 3 independent assays. *Htr* knockdown efficiency was confirmed by RT PCR. **b** High expression of *Htr2a* and *Htr3a* in intestinal macrophage cells, which were enriched via FACS. **c** PGE2 production in macrophages treated with indicated inhibitors of 5-HT receptor. 10 μg/mL Ketanserin and 25 μg/mL Tropisetron were used and 3 independent experiments were performed. **d** ELISA detection for PGE2 production in microphages, which were sorted from 5-HT treated *Htr2a* KO, *Htr3a* KO, or DKO mice. All PGE2 levels were normalized to those of Vehicle treated mice ($n = 3$ per group). **e** Fluorescence staining of intestinal tissue from 2-month-old *Lgr5*[GFP], *Lgr5*[GFP];*Htr2a*^{−/−}, *Lgr5*[GFP];*Htr3a*^{−/−}, and *Lgr5*[GFP];*Htr2a*^{−/−};*Htr3a*^{−/−} mice. 100 fields from five mice were observed. **f, g** FACS detection for ISC ratios in SI or colon tissues from dmPGE2-treated (**f**) or indomethacin (Indo)-treated (**g**) mice. 5 mg/kg dmPGE2, 10 mg/kg indo and 150 mg/kg pCPA were intraperitoneally injected and 5 mice were used per group. **h** Organoid formation of ISCs, supplemented with/without 1 μM dmPGE2. Typical organoid images of three independent assays were shown. **i** PGE2 expression was analyzed in CSF1R^{+} macrophage cells, which were obtained from SI tissues of SPF, GF, GF + FMT, and GF + VA mice. 5 mice were used for each group. Typical FACS results were shown in the left panel, and PGE2^{+} macrophage ratios were in the right panel. **j** PGE2^{+} macrophages were isolated from ileum tissues of CD45.1 mice, and transferred to *Lgr5*[GFP] mice, and SI tissue location of CD45.1[+] macrophages was shown. 2×10^6 live PGE2^{+} macrophages were used for each mouse. **k** PGE2^{+} macrophage-transfer assay was performed to GF-*Lgr5*[GFP] mice and DT-treated *Lgr5*[GFP]*Tph2*[DTR] mice, and ISC ratios were measured with FACS. SI and colon tissues were measured. $n = 5$ mice per group. *$P < 0.05$, **$P < 0.01$, ***$P < 0.001$ by unpaired one-tailed Student's *t*-test; ns, not significant.

(#ab2318) antibody was from Abcam. HRP-conjugated secondary antibodies were from Sungene Biotech. Alexa-594, Alexa-488, and Alexa-647-conjugated anti-rabbit and anti-mouse secondary antibodies were purchased from Invitrogen. OpalTM 7-color fIHC kit (#MEL797001KT) was from PerKinElmer. Polymer HRP detection kits were from GBI labs. N2 supplement and B27 supplement were from Invitrogen. Wnt3a, RSPO1, Noggin and EGF proteins were purchased from Peprotech. N2 and B27 were from Invitrogen. 4′,6-diamidino-2-phenylindole (DAPI), N-acetylcysteine, Y27632 and hyaluronidase were from Sigma-Aldrich. Riluzole, Primidone, pCPA, and Atractylodin were purchased from MedChemExpress (MCE). Chlorpromazine was obtained from Selleck Chemicals.

Generation of knockout mice by CRISPR/Cas9 technology
Sert^{−/−}, *Tph1*^{−/−}, *Htr2a*^{−/−}, *Htr3a*^{−/−}, *Ptges*^{−/−}, *Ptger1*^{−/−}, *Ptger4*^{−/−}, *Tph1*[DTR], and *Tph2*[DTR] mice were generated using CRISPR/Cas9 approaches as described.[64] Approximate 250 zygotes in C57BL/6 background were injected with corresponding sgRNAs (Supplementary information, Table S2) and subsequently transferred to the uterus of pseudo-pregnant ICR females, from which viable founder mice were obtained. *Tph2*-KO mice were obtained from Feng Liu Lab. All mouse genotypes were verified by DNA sequencing. Other gene-modified mouse strains were: *Rosa26*[lsl-Cas9] mice were purchased from the Jackson Laboratory. *Lgr5*[GFP-CreERT2] mice were obtained from Model Animal Research Center of Nanjing University. *Rosa26*[YFP] mice were purchased from Shanghai Biomodel Organism Science & Technology Development Co., Ltd. *Rosa26*[lacZ] mice were from Shanghai Bioray Laboratory. *Axin2*[lacZ] and *Apc*[min/+] mice were from Nanjing Biomedical Research Institute of Nanjing University. All the mouse strains were C57BL/6 background and maintained under specific pathogen free conditions with approval by the Institutional Committee of Institute of Biophysics, Chinese Academy of Sciences. The study is compliant with all relevant ethical regulations regarding animal research. For TAM injection, 200 μL TAM in sunflower oil (10 μg/μL) was intraperitoneally injected into *Lgr5*[CreERT2] mice at 60 days old.

All SPF mice, including WT C57BL/6, were bred and housed in a barrier facility accredited by the Institutional Committee of Institute of Biophysics, Chinese Academy of Sciences and Zhengzhou University. GF C57BL/6 J mice were maintained in GF conditions in vinyl isolators in the animal facility of Institute of Laboratory Animal Science, Chinese Academy of Medical Sciences and were used according to protocols approved by the Institutional Committee of Institute of Biophysics, Chinese Academy of Sciences.

Tyramide signal amplification for FISH
For multiple-color staining, OpalTM 7-color fIHC kit was used according to the manual. Briefly, intestine paraffin sections were sequentially stained with Anti-GFP, anti-Krt20, anti-Ki67, anti-OLFM4 and anti-E-Cad primary antibodies, and HRP-conjugated secondary antibodies. One of the six Opal reagents were used for staining, followed by microwave treatment and another round staining. Opal520, Opal540, Opal570, Opal620, Opal650, Opal690 dyes were used for staining. Samples were visualized using Vectra Automated Quantitative Pathology Imaging System (PerkinElmer).

Organoid culture and co-culture
For intestinal organoid culture, murine intestines were digested by 0.1% type-I collagenase (Invitrogen), and further incubated in 1× TrypLE express (Life

Technologies) supplemented with 0.8 kU/mL DNaseI (Roche) for single cell preparation. Lgr5^{+} cells were sorted using FACS. Intestinal organoid medium was used as previously described with minor modifications.[2] Briefly, Dulbecco's modified Eagle's medium/F12 medium (Invitrogen) was supplemented with 20 ng/mL EGF (Peprotech), 100 ng/mL Noggin, N2 (Invitrogen), B27 (Invitrogen), 1.25 mM N-acetylcysteine (Sigma-Aldrich), 1 mg/mL Rspo1 (peprotech), 20 mM Y27632 (Sigma-Aldrich). Medium was replaced every 2 days and pictures of organoids were taken 1 week later. For ISC-immune cell co-culture, ISC and CD45^{+} immune cells were co-cultured at ratio 1:10, and cultured ISC medium supplemented with 1000 U/mL murine IL-2, 10 ng/mL murine IL-15, 50 ng/mL murine IL-7 and 5 μM 5-HT.

Isolation of intestinal macrophages and enteric serotonergic neurons
For intestinal macrophage isolation, small intestines were washed with three times with PBS, and then were opened longitudinally, cut into 1-cm pieces, and incubated in PBS supplemented with 5 uM EDTA, 5%FBS and 1 mM DTT. Then the samples were digested with 0.14 U/mL Liberase (Sigma) for 30 min at 37 °C on a rotor. The digested cell suspension was then passed through 70 mm cell strainers, followed by FACS staining and CD11b^{+}F480^{+}CX3CR1^{+} intestinal macrophages were sorted via FACS Aria III (BD).

For enteric serotonergic neuron isolation, myenteric plexus was isolated and dissociated in M199 medium (Invitrogen) containing 1.1 mg/mL collagenase, 50 U/mL DNase I, 0.1% BSA, 1 mM CaCl2, 20 mM Hepes for 40 min at 37 °C. Then single cells were fixed, penetrated and stained with Tph2 antibody, and Tph2^{+} serotonergic neuron can be sorted by FACS.

β-galactosidase staining for ISC tracing
For ISC tracing, 60-day-old *Lgr5*[GFP-IRES-CreERT2]; *Rosa26*[lsl-lacZ] (*LR*[lacZ]) mice were intraperitoneally injected with 2 mg TAM in sunflower oil (10 μg/μL). On day 61, day 63, day 65 and day 90, 8 mice in one group were sacrificed and intestine tissues were obtained for β-galactosidase staining (Beyotime Biotechnology, #RG0039). Briefly, intestines were incubated in fixation buffer (RG0039-1) at room temperature for 20 min and then washed with PBS. Samples were incubated in staining buffer (including 10 μL buffer A, 10 μL buffer B, 930 μL buffer C and 50 μL X-Gal) at 37 °C for 30 min, and the samples were then screened by EPSON ImageScanner III. Finally the traced units were counted.

Treatment with neurotransmitter antagonists and metabolites
For neurotransmitter analysis, *Lgr5*[GFP] mice were intraperitoneally injected with neurotransmitter antagonists according to standard dosages (Riluzole, 25 mg/kg; Primidone, 100 mg/kg; pCPA, 150 mg/kg; Chlorpromazine 5 mg/kg; Atractylodin 1 mg/kg), and crypts of small intestine and colon were collected for ISC detection.

For neurotransmitter analysis, GF mice were treaded with indicated metabolites daily for 5 days, followed by *Tph2*-detection. The dosages are determined as previously described: VA, 50 mg/kg; Pipecolic acid, 250 mg/kg; sarcosine, 300 mg/kg; 1, 4-MeImAA, 20 mg/kg; 5-Aminovaleric acid, 20 mg/kg; Trimethylamine Noxide, 20 mg/kg; S-Lactoylglutathione, 50 mg/kg; Adenine, 50 mg/kg; Prostaglandin E2, 1 mg/kg; N-Acetylglutamic acid, 150 mg/kg; N-Acetylornithine, 50 mg/kg; Betaine aldehyde, 30 mg/kg.
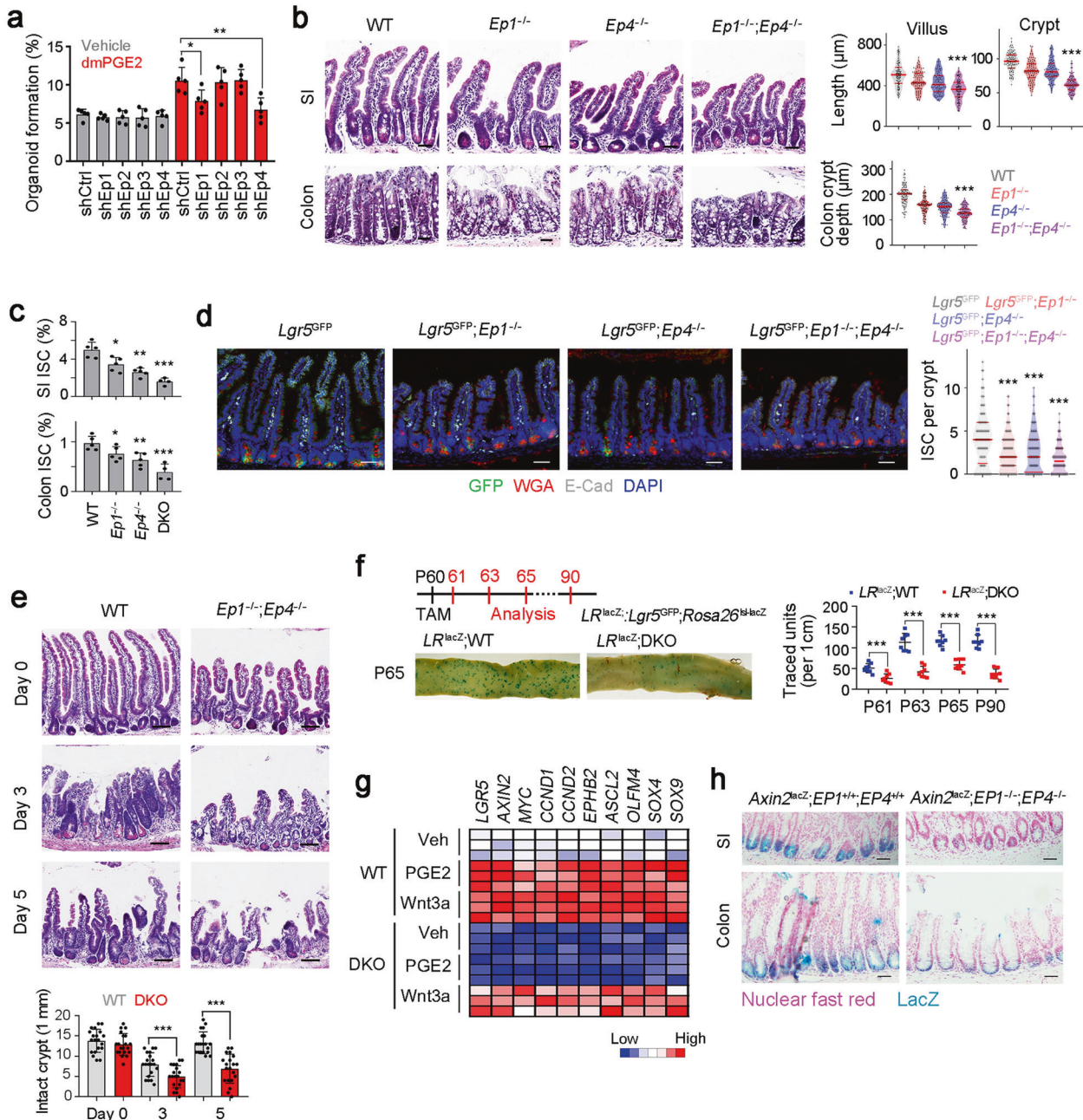
Fig. 7 PGE2 drives Wnt signaling activation to maintain ISC stemness. a Organoid formation assay of indicated PGE2 receptor-silenced ISCs, supplemented with 1 μM dmPGE2. Results are from 5 independent experiments. **b** H&E staining of SI and colon of WT, *Ep1*−/−, *Ep4*−/−, and DKO mice. Typical images were shown in left panel and 100 fields from five mice were observed in right panel. Scale bars, 50 μm. **c** FACS detection for ISC ratios in SI and colon crypt, which were from WT, *Ep1*−/−, *Ep4*−/−, and DKO mice. 5 mice per group. **d** Fluorescence staining of intestinal tissue from 2-month-old *Lgr5*GFP, *Lgr5*GFP;*Ep1*−/−, *Lgr5*GFP;*Ep4*−/− and *Lgr5*GFP;*Ep1*−/−;*Ep4*−/− mice. 100 fields from five mice were observed. Scale bars, 50 μm. **e** WT and DKO mice were treated with 10 Gy's radiation, and sacrificed at indicated time points, and typical images were shown. 20 fields from five mice for each group. Scale bars, 100 μm. **f** *Lgr5*GFP-CreERT2; *Rosa26*lsl-lacZ (*LR*lacZ) mice were crossed with DKO mice, and intestinal whole-mount staining of β-gal was performed for lineage tracing analysis. 8 mice were observed for each group and typical sections were shown. P60, postnatal day 60; TAM, tamoxifen. **g** Heatmap of indicated Wnt/β-catenin target genes in WT and DKO ISCs. 3 mice were used per group. **h** WT and DKO mice were crossed with *Axin2*lacZ mice. SI and colon tissues were stained for β-gal expression. β-gal staining indicates the activation of Wnt/β-catenin signaling. Typical images of 5 mice were shown. Scale bars, 50 μm. *P < 0.05, **P < 0.01, ***P < 0.001 by unpaired one-tailed Student's *t*-test. At least three independen*t* repeats were performed for each experiment and the representative results were shown.

In situ hybridization and FISH

For Lgr5 in situ hybridization, mouse *Lgr5* gene was cloned into PCDNA4 plasmid and in situ probes targeting 1 kb N-terminal fragment of mouse *Lgr5* were labeled with Digoxin through in vitro transcription.[65] Intestinal sections were rehydrated, treated with 0.2 M HCl and proteinase K solution, and then incubated in acetic anhydride solution, followed by hybridization overnight at 68 °C with *Lgr5* probes in hybridization buffer (5× standard saline citrate (SSC, pH 4.5), 2% blocking powder (Roche), 50 μg/mL yeast transfer RNA, 50% formamide, 5 mmol/L ethylenediaminetetraacetic acid, 0.05% 3[3-cholamino-propyl diethylammonio]-1-propane sulfonate, 50 μg/mL heparinm, 0.1%

Tween 20). Samples were then rinsed in 2× SSC and washed with 2× SSC/50% formamide at 60 °C for 3 × 20 min. Then sections were blocked for 30 min in TBST containing 0.5% blocking powder (Roche), followed by overnight incubation at 4 °C in blocking solution with HRP-conjugated anti-digoxigenin (1:2000 dilution; Roche).

CRISPR affinity purification in situ of regulatory elements
CRISPR affinity purification in situ of regulatory elements (CAPTURE) assay was performed to as described.[39,66] Briefly, pEF1a-BirA-V5-neo (Addgene #100548) pEF1a-FB-dCas9-puro (Addgene #100547) and *Tph2* promoter were over-expressed for intracellular dCas9 biotinylation and purified with Streptavidin, and the enrichment of *Tph2* promoter binding proteins were identified through silver staining and mass spectrum, and confirmed by western blot.

Western blot
ISCs or myenteric plexus cells were lyzed with RIPA buffer (150 mM NaCl, 0.1% SDS, 1% NP40, 0.5% sodium deoxycholate, 1 mM EDTA, 50 mM Tris, pH 8.0) and separated with SDS-PAGE. Then samples were then transferred to NC membrane (Beyotime Biotechnology, Shanghai, China) and incubated with primary antibodies. After washing with TBST three times, membranes were incubated with HRP-conjugated secondary antibodies for visualization.[67]

PGE2 secretion assay
We established PGE2 secretion assay to sort viable PGE2$^+$ cells. Streptavidin-conjugated CD45 antibody (Abcore, #AC12-0147-22) and Biotin-conjugated PGE2 antibody (Fine Biotech, #EU2554) were mixed at a mole ratio of 1:1 for 10 min, and then subjected to the incubation with samples and the PGE2-catching antibody was attached to CD45$^+$ immunocytes. The cells were then placed in 37 °C for 45 min to facilitate PGE2 secretion, and then samples were labeled with another PGE2 antibody (Abcam, #ab2318) for PGE2 detection. Other antibodies could also be used for co-staining for FACS or immunofluorescence.

Macrophage depletion
For macrophage depletion, 200 µg neutralizing antibodies to CSF1R (#M279; Amgen) or control rat IgG were administered intraperitoneally every 3 days for 1 month. Efficiency of macrophage depletion was confirmed by FACS 3 days after antibody injection, and then ISC numbers and functions were analyzed.

ChIP
ChIP was performed according to the standard protocol (Upstate Biotechnology, Inc.). Briefly, myenteric plexus cells were fixed in 1% formaldehyde for 10 min at 37 °C, and then cracked by SDS lysis buffer for 10 min on ice, followed by ultrasonic to shear DNA into fragments between 200 bp and 500 bp. Anti-HDAC1, anti-HDAC2, anti-H4K5ac, anti-H3K9ac, and anti-H3K4me3 antibodies were used for ChIP assays as described.[68]

TOPFLash
TOPFlash assay was used for Wnt/β-catenin activation detection. TOPFlash (Plasmid #12456, Addgene) and FOPFlash (Plasmid #12457, Addgene) were transfected into ISCs (1×10^5) along with thymidine kinase through electroporation, followed by 36 h incubation in organoid formation medium. Then cells were lyzed and detected using substrates L and S (Promega dual luciferase kit). Wnt/β-catenin activation was measured by fold changes of TOPFlash versus FOPFlash as control.

Realtime PCR
Total RNA was extracted from ISCs or myenteric plexus cells, and used for reverse transcription PCR (RT-PCR). Complement DNA (cDNA) was used as templates for realtime PCR.[69] Sequence-specific primers for detected genes were listed in Supplementary information, information, Table S3.

Co-immunoprecipitation (co-IP) assay
For co-IP, samples were lyzed with RIPA buffer for 30 min at 4 °C and precipitate was removed from cell lysates by centrifugation at $12,000 \times g$ for 10 min. Supernatants were pre-cleared by protein A/G beads (Santa Cruz Biotechnology) for 1 h, and anti-HTR1B, anti-Axin1 or anti-β-catenin antibody was added for 4 h incubation. New protein A/G beads were added for immunoprecipitation. Precipitates were collected and examined by estern blot with indicated antibodies.

Statistics and reproducibility
For statistical evaluation, an unpaired Student's t-test was applied for calculating statistical probabilities in this study. For all panels, at least three independent experiments were performed with similar results, and representative experiments are shown. Data were analyzed by GraphPad Prism 5.0. Kaplan–Meier survival analysis was performed by SPSS 20.0. All flow cytometry data were analyzed with FlowJo 10 (Treestar). Adobe Photoshop CC 14.0 and ImageJ 1.48 were used for figure presentation. One-tailed unpaired Student's t-test was performed using Excel 2010. P-values ≤ 0.05 were considered significant (*P < 0.05; **P < 0.01; ***P < 0.001); non-significant (NS), P > 0.05.

DATA AVAILABILITY
All other data supporting the findings of this study are available from the corresponding author on reasonable request.

REFERENCES
1. Gehart, H. & Clevers, H. Tales from the crypt: new insights into intestinal stem cells. *Nat. Rev. Gastro. Hepat.* **16**, 19–34 (2019).
2. Sato, T. et al. Single Lgr5 stem cells build crypt-villus structures in vitro without a mesenchymal niche. *Nature* **459**, 262–265 (2009).
3. Hu, D., Yan, H., He, X. C. & Li, L. Recent advances in understanding intestinal stem cell regulation. *F1000Research* **8**, 16793.1 (2019).
4. Zhu, P. P. et al. LncGata6 maintains stemness of intestinal stem cells and promotes intestinal tumorigenesis. *Nat. Cell Biol.* **20**, 1134–1145 (2018).
5. Barker, N. et al. Identification of stem cells in small intestine and colon by marker gene Lgr5. *Nature* **449**, 1003–1007 (2007).
6. Sato, T. et al. Paneth cells constitute the niche for Lgr5 stem cells in intestinal crypts. *Nature* **469**, 415–418 (2011).
7. Rodriguez-Colman, M. J. et al. Interplay between metabolic identities in the intestinal crypt supports stem cell function. *Nature* **543**, 424–435 (2017).
8. Yilmaz, O. H. et al. mTORC1 in the Paneth cell niche couples intestinal stem-cell function to calorie intake. *Nature* **486**, 490–495 (2012).
9. Shoshkes-Carmel, M. et al. Subepithelial telocytes are an important source of Wnts that supports intestinal crypts. *Nature* **557**, 242–254 (2018).
10. Wu, N. et al. MAP3K2-regulated intestinal stromal cells define a distinct stem cell niche. *Nature* **592**, 606–610 (2021).
11. McCarthy, N., Kraiczy, J. & Shivdasani, R. A. Cellular and molecular architecture of the intestinal stem cell niche. *Nat. Cell Biol.* **22**, 1033–1041 (2020).
12. Santos, A. J. M., Lo, Y. H., Mah, A. T. & Kuo, C. J. The intestinal stem cell niche: homeostasis and adaptations. *Trends Cell Biol.* **28**, 1062–1078 (2018).
13. Fu, Y. Y. et al. T cell recruitment to the intestinal stem cell compartment drives immune-mediated intestinal damage after allogeneic transplantation. *Immunity* **51**, 90–102 (2019).
14. Lindemans, C. A. et al. Interleukin-22 promotes intestinal-stem-cell-mediated epithelial regeneration. *Nature* **528**, 560–564 (2015).
15. Zhu, P. et al. IL-13 secreted by ILC2s promotes the self-renewal of intestinal stem cells through circular RNA circPan3. *Nat. Immunol.* **20**, 183–194 (2019).
16. Spencer, N. J. & Hu, H. Z. Enteric nervous system: sensory transduction, neural circuits and gastrointestinal motility. *Nat. Rev. Gastro. Hepat.* **17**, 338–351 (2020).
17. Margolis, K. G., Cryan, J. F. & Mayer, E. A. The microbiota-gut-brain axis: from motility to mood. *Gastroenterology* **160**, 1486–1501 (2021).
18. Sahu, A. et al. The 5-Hydroxytryptamine signaling map: an overview of serotonin-serotonin receptor mediated signaling network. *J. Cell Commun. Signal.* **12**, 731–735 (2018).
19. Gutknecht, L., Kriegebaum, C., Waider, J., Schmitt, A. & Lesch, K. P. Spatio-temporal expression of tryptophan hydroxylase isoforms in murine and human brain: convergent data from Tph2 knockout mice. *Eur. Neuropsychopharm.* **19**, 266–282 (2009).
20. Hoyer, D., Hannon, J. P. & Martin, G. R. Molecular, pharmacological and functional diversity of 5-HT receptors. *Pharmacol. Biochem. Behav.* **71**, 533–554 (2002).
21. Sumara, G., Sumara, O., Kim, J. K. & Karsenty, G. Gut-derived serotonin is a multifunctional determinant to fasting adaptation. *Cell Metab.* **16**, 588–600 (2012).
22. Crane, J. D. et al. Inhibiting peripheral serotonin synthesis reduces obesity and metabolic dysfunction by promoting brown adipose tissue thermogenesis. *Nat. Med.* **21**, 166–172 (2015).
23. Zmora, N., Suez, J. & Elinav, E. You are what you eat: diet, health and the gut microbiota. *Nat. Rev. Gastro. Hepat.* **16**, 35–56 (2019).
24. Jiao, Y. H., Wu, L., Huntington, N. D. & Zhang, X. Crosstalk between gut microbiota and innate immunity and its implication in autoimmune diseases. *Front. Immunol.* **11** e282 (2020).
25. Wong, S. H. & Yu, J. Gut microbiota in colorectal cancer: mechanisms of action and clinical applications. *Nat. Rev. Gastro. Hepat.* **16**, 690–704 (2019).

26. Sommer, F. & Backhed, F. The gut microbiota-masters of host development and physiology. *Nat. Rev. Microbiol.* **11**, 227–238 (2013).

27. Savage, D. C., Siegel, J. E., Snellen, J. E. & Whitt, D. D. Transit time of epithelial cells in the small intestines of germfree mice and ex-germfree mice associated with indigenous microorganisms. *Appl. Environ. Microbiol.* **42**, 996–1001 (1981).

28. Alam, M., Midtvedt, T. & Uribe, A. Differential cell kinetics in the ileum and colon of germfree rats. *Scand. J. Gastroentero.* **29**, 445–451 (1994).

29. Lee, Y. S. et al. Microbiota-derived lactate accelerates intestinal stem-cell-mediated epithelial development. *Cell Host Microbe* **24**, 833–846 (2018).

30. Ooijevaar, R. E., Terveer, E. M., Verspaget, H. W., Kuijper, E. J. & Keller, J. J. Clinical application and potential of fecal microbiota transplantation. *Annu. Rev. Med.* **70**, 335–351 (2019).

31. Metcalfe, C., KIjavin, N. M., Ybarra, R. & de Sauvage, F. J. Lgr5(+) stem cells are indispensable for radiation-induced intestinal regeneration. *Cell Stem Cell* **14**, 149–159 (2014).

32. Porvasnik, S. L, Mah, C., & Polyak, S. Targeting murine small bowel and colon through selective superior mesenteric artery injection. *Microsurgery* **30**, 487–493 (2010).

33. Gross, E. R., Gershon, M. D., Margolis, K. G., Gertsberg, Z. V. & Cowles, R. A. Neuronal serotonin regulates growth of the intestinal mucosa in mice. *Gastroenterology* **143**, 408–417 (2012).

34. Gershon, M. D. & Tack, J. The serotonin signaling system: From basic understanding to drug development-for functional GI disorders. *Gastroenterology* **132**, 397–414 (2007).

35. Chen, H. W. et al. A forward chemical genetic screen reveals gut microbiota metabolites that modulate host physiology. *Cell* **177**, 1217–1231 (2019).

36. Matsumoto, M. et al. Colonic absorption of low-molecular-weight metabolites influenced by the intestinal microbiome: a pilot study. *PLoS One* **12**, e0169207 (2017).

37. Luu, M. et al. Microbial short-chain fatty acids modulate CD8(+) T cell responses and improve adoptive immunotherapy for cancer. *Nat. Commun.* **12**, 4077 (2021).

38. Zhang, Y. et al. Analysis of the NuRD subunits reveals a histone deacetylase core complex and a connection with DNA methylation. *Genes Dev.* **13**, 1924–1935 (1999).

39. Liu, X. et al. In situ capture of chromatin interactions by biotinylated dCas9. *Cell* **170**, 1028–1043 (2017). e1019.

40. Ekwall, K. Genome-wide analysis of HDAC function. *Trends Genet.* **21**, 608–615 (2005).

41. Benayoun, B. A. et al. H3K4me3 breadth is linked to cell identity and transcriptional consistency. *Cell* **163**, 1281–1264 (2015).

42. Brun, P. & Akbarali, H. I. Culture of neurons and smooth muscle cells from the myenteric plexus of adult mice. *Methods Mol. Biol.* **1727**, 119–125 (2018).

43. Roulis, M. et al. Paracrine orchestration of intestinal tumorigenesis by a mesenchymal niche. *Nature* **580**, 524–529 (2020).

44. Grainger, J. R. et al. Inflammatory monocytes regulate pathologic responses to commensals during acute gastrointestinal infection. *Nat. Med.* **19**, 713–721 (2013).

45. Ulmann, L., Hirbec, H. & Rassendren, F. P2X4 receptors mediate PGE2 release by tissue-resident macrophages and initiate inflammatory pain. *EMBO J.* **29**, 2290–2300 (2010).

46. De Schepper, S. et al. Self-maintaining gut macrophages are essential for intestinal homeostasis. *Cell* **176**, 676–676 (2019).

47. Gabanyi, I. et al. Neuro-immune interactions drive tissue programming in intestinal macrophages. *Cell* **164**, 378–391 (2016).

48. Barker, N. Adult intestinal stem cells: critical drivers of epithelial homeostasis and regeneration. *Nat. Rev. Mol. Cell Bio* **15**, 19–33 (2014).

49. Sikander, A., Rana, S. V. & Prasad, K. K. Role of serotonin in gastrointestinal motility and irritable bowel syndrome. *Clin. Chim. Acta.* **403**, 47–55 (2009).

50. Chen, Z. et al. LncFZD6 initiates Wnt/beta-catenin and liver TIC self-renewal through BRG1-mediated FZD6 transcriptional activation. *Oncogene* **37**, 3098–3112 (2018).

51. Chen, Z., Yao, L., Liu, Y. & Zhu, P. LncTIC1 interacts with beta-catenin to drive liver TIC self-renewal and liver tumorigenesis. *Cancer Letters* **430**, 88–96 (2018).

52. Zhu, P. et al. lnc-beta-Catm elicits EZH2-dependent beta-catenin stabilization and sustains liver CSC self-renewal. *Nat. Struct. Mol. Biol.* **23**, 631–639 (2016).

53. Na, Y. R. et al. Prostaglandin E2 receptor PTGER4-expressing macrophages promote intestinal epithelial barrier regeneration upon inflammation. *Gut* **70**, 2249–2260 (2021).

54. Na, Y. R., Stakenborg, M., Seok, S. H. & Matteoli, G. Macrophages in intestinal inflammation and resolution: a potential therapeutic target in IBD. *Nat. Rev. Gastro. Hepat.* **16**, 531–543 (2019).

55. Sehgal, A. et al. The role of CSF1R-dependent macrophages in control of the intestinal stem-cell niche. *Nat. Commun.* **9**, 1272 (2018).

56. Chng, S. H. et al. Ablating the aryl hydrocarbon receptor (AhR) in CD11c+ cells perturbs intestinal epithelium development and intestinal immunity. *Sci. Rep.* **6**, 23820 (2016).

57. D'Angelo, F. et al. Macrophages promote epithelial repair through hepatocyte growth factor secretion. *Clin. Exp. Immunol.* **174**, 60–72 (2013).

58. Glatzle, J. et al. Expression of 5-HT3 receptors in the rat gastrointestinal tract. *Gastroenterology* **123**, 217–226 (2002).

59. Lavelle, A. & Sokol, H. Gut microbiota-derived metabolites as key actors in inflammatory bowel disease. *Nat. Rev. Gastro. Hepat.* **17**, 223–237 (2020).

60. Round, J. L. & Mazmanian, S. K. The gut microbiota shapes intestinal immune responses during health and disease. *Nat. Rev. Immunol.* **9**, 313–323 (2009).

61. Kim, C. H., Park, J. & Kim, M. Gut microbiota-derived short-chain fatty acids, T cells, and inflammation. *Immune Network* **14**, 277–288 (2014).

62. Kaiko, G. E. et al. The colonic crypt protects stem cells from microbiota-derived metabolites. *Cell* **165**, 1708–1720 (2016).

63. Chikina, A. S. et al. Macrophages maintain epithelium integrity by limiting fungal product absorption. *Cell* **183**, 411–428 (2020).

64. Zhu, X. X. et al. An efficient genotyping method for genome-modified animals and human cells generated with CRISPR/Cas9 System. *Sci Rep.* **4**, 6420 (2014).

65. Chen, Z., Wu, J. & Liu, B. Identification of cis-HOX-HOXC10 axis as a therapeutic target for colorectal tumor-initiating cells without APC mutations. *Cell Rep.* **36**, 109431 (2021).

66. Chen, Z. et al. circular RNA cia-MAF drives self-renewal and metastasis of liver tumor-initiating cells via transcription factor MAFF. *J. Clin. Invest* **131**, e148020 (2021).

67. Zhu, P. P. et al. LncBRM initiates YAP1 signalling activation to drive self-renewal of liver cancer stem cells. *Nat. Commun.* **7**, 13608 (2016).

68. Zhu, P. P. et al. ZIC2-dependent OCT4 activation drives self-renewal of human liver cancer stem cells. *J. Clin. Invest.* **125**, 3795–3808 (2015).

69. Chen, Z. Z. et al. LncSox4 promotes the self-renewal of liver tumour-initiating cells through Stat3-mediated Sox4 expression. *Nat. Commun.* **7**, 12598 (2016).

ACKNOWLEDGEMENTS

AUTHOR CONTRIBUTIONS

P.Z. designed and performed experiments, analyzed data, and wrote the paper; J.W. and T.L. performed experiments and analyzed data; D.F. and X.Z. generated genome modified mice; F.L. provided *Tph2* KO mice; B.L., H.G., and Y.D. performed some experiments; Y.T. initiated and analyzed data; Z.F. initiated the study, organized, designed, and wrote the paper.

COMPETING INTERESTS

The authors declare no competing interests.

ADDITIONAL INFORMATION

Supplementary information, information The online version contains supplementary material available at https://doi.org/10.1038/s41422-022-00645-7.

Correspondence and requests for materials should be addressed to Pingping Zhu, Yong Tian or Zusen Fan.

Reprints and permission information is available at http://www.nature.com/reprints